Promoting axon regeneration by enhancing the non-coding function of the injury-responsive coding gene *Gpr151*

Bohm Lee[#1], Jinyoung Lee[#1], Yewon Jeon[#1], Hyemin Kim[1], Minjae Kwon[1], Jung Eun Shin[1,2] and Yongcheol Cho[*1]

[1] Department of Life Sciences, Korea University, Seoul 02841, Republic of Korea

[2] Department of Molecular Neuroscience, Dong-A University College of Medicine, Busan 49201, Republic of Korea

[#]These authors contributed equally to this work.

*Correspondence to: **Yongcheol Cho**, Department of Life Sciences, Korea University, Anam-ro 145, Seongbuk-gu, Seoul 02841, Republic of Korea. Phone: +82 2 3920 4727, Email: ycho77@korea.ac.kr

Abstract

Gene expression profiling in response to nerve injury has been mainly focused on protein functions of coding genes to understand mechanisms of axon regeneration and to identify targets of potential therapeutics for nerve repair. However, the protein functions of several highly injury-induced genes including *Gpr151* for regulating the regenerative ability remain unclear. Here we present an alternative approach focused on non-coding functions of the coding genes, which led to the identification of the non-coding function of *Gpr151* RNA interacting with RNA-binding proteins such as CSDE1. *Gpr151* promotes axon regeneration by the function of its 5'- untranslated region (5'UTR) and expression of an engineered form of the 5'UTR improves regenerative capacity in vitro and in vivo in both sciatic nerve and optic nerve injury models. Our data suggest that searching injury-induced coding genes potentially functioning by their non-coding regions is required for the RNA-based gene therapy for improving axon regeneration.

Keywords: 5'UTR, axotomy, axon regeneration, RNA-binding protein, translation, *GPR151*, single-exon gene, CSDE1, dorsal root ganglion, *RiboTag*

Introduction

Neurons in the peripheral nervous system (PNS) activate the intrinsic regeneration program after axons are injured, a process that is controlled by the expression of injury-responsive genes (He and Jin, 2016; Liu et al., 2011; Mahar and Cavalli, 2018; Shin and Cho, 2017; Smith and Skene, 1997; Sun and He, 2010) Comparative analysis of transcriptomic data between naïve and regenerating sensory neurons in dorsal root ganglia (DRG) has revealed a number of differentially expressed genes (DEGs), within which there is a subgroup of regeneration-associated genes that are required for successful regeneration (Blackmore, 2012; Ma and Willis, 2015). However, the molecular mechanisms of the particular regeneration-associated genes involved in the regulation of regenerative potential have not been clearly delineated.

Functional analysis of protein-coding DEGs is generally regarded as a reliable strategy for understanding cellular mechanisms. This paradigm requires proof that upregulated protein-coding mRNA is directed to ribosome complexes if it is believed that the function of DEGs results primarily from the resulting proteins. However, with respect to the IRGs, several reports have shown a poor correlation between their mRNA and protein levels (Gunawardana and Niranjan, 2013; Huang et al., 2009; Reinhold et al., 2015; Terman, 1970), indicating that it is necessary to study the differentially expressed mRNA without the assumption that their function as regeneration-associated genes is dependent on their protein products. Therefore, monitoring the fate of the mRNA itself may be the primary route to correctly understanding how neurons alter their physiology to enter a regenerative state via DEGs (Gygi et al., 1999; Koussounadis et al., 2015; Liu et al., 2016; Maier et al., 2009).

RNA-binding proteins (RBPs) play various roles including the regulation of RNA for its stability, translational efficiency, modification, localization and intermolecular interaction (Hentze et al., 2018; Van Nostrand et al., 2020). RBPs such as the CELF family protein UNC-75 affect axon regeneration in *C. elegans* via regulating alternative splicing and the Zipcode-binding protein ZBP1 can promote nerve regeneration in mice by regulating axonal mRNA transport (Chen et al., 2016; Donnelly et al., 2011). Recent studies have shown that mRNA differentially expressed by specific cues can be directed to RBPs and modulate their regulatory functions (Kumari and Sampath, 2015;

Sampath and Ephrussi, 2016). These reports raise a hypothesis that the injury-dependent mRNA may affect the regenerative program by regulating RBPs independently from the function of its translated protein.

In this study, we conducted a comparative analysis of transcriptomes under an axon regeneration paradigm based on their ribosome-association efficiency using *RiboTag* mice after axonal injury (Sanz et al., 2009). We found that a group of injury-responsive genes exhibited no increase in their ribosome-association efficiency even when their mRNA was dramatically upregulated after axonal injury, supporting potential non-coding functions of these mRNA. Of these genes, *Gpr151* encodes an orphan G protein-coupled receptor (GPCR) that is implicated in neuropathic pain and nicotine addiction (Antolin-Fontes et al., 2020; Holmes et al., 2017; Jiang et al., 2018). Because *Gpr151* is a single-exon protein-coding gene, it was selected to explore the mRNA function by examining a single form of transcript, avoiding a need to consider alternatively spliced isoforms. We found that the 5' untranslated region (5'UTR) of *Gpr151* mRNA promotes axon regeneration and identified RBPs interacting with the 5'UTR, including CSDE1, which was found to be a negative regulator of axonal regrowth in vitro. Moreover, we found that expressing an engineered form of the 5'UTR showed improved CSDE1-association and enhanced axon regeneration both in vitro and in vivo. Overexpression of the engineered 5'UTR did not significantly change the transcriptomic profiles but instead modulated the pool of CSDE1-associated RNA and promoted the release of RNA from CSDE1, including ribosomal protein-encoding mRNA. Finally, we retrospectively re-analyzed our previous transcriptomic data to present another example of injury-responsive mRNA with the non-coding function, finding that *Sox11* mRNA is potentially involved in regulating axon regeneration. In this study, we introduce a new approach to DEG analysis by incorporating ribosome-association efficiency data from an axon regeneration paradigm and uncover the role of protein-coding mRNA as a biological modulator of the RBP function.

Results

Gpr151 is an injury-responsive protein-coding gene that is not directed to ribosome

To identify regeneration-associated genes (RAGs) regulating regeneration by their non-coding functions, *RiboTag* mice were crossed with *Advillin*-Cre mice and utilized to specifically isolate the ribosome complex-bound RNA from the dorsal root ganglia (DRG) with or without sciatic nerve axotomy (Figures 1A, 1B and S1) (Ma and Willis, 2015; Sanz et al., 2009; Zurborg et al., 2011). Comparative analysis between the whole transcriptome and the ribosome-bound RNA showed that a large portion of upregulated coding genes was not directed to ribosome complex, suggesting that non-coding functions of these need to be investigated (Figure 1C). Among them, we selected *Gpr151* as a model gene, an orphan G protein-coupled receptor that mediates nicotine sensitivity and neuropathic pain (Antolin-Fontes et al., 2020; Broms et al., 2015, 2017; Jiang et al., 2018). While *Gpr151* upregulation after nerve injury has been reported by several transcriptome studies using DRG tissues 12–16, its role in the regulation of axon regeneration remains unknown (Marvaldi et al., 2020; Shin et al., 2019; Tedeschi et al., 2017; Wlaschin et al., 2018; Wu et al., 2016). We found that *Gpr151* mRNA was dramatically upregulated with no changes in the ribosome-association after sciatic nerve injury (Figure 1D). Moreover, the average FPKM read count of *Gpr151* reached over 2,000 at 24 hours after injury with a further increase at 72 hours, indicating the abundance of this RNA (Figure S2) 13. Western blot analysis, qPCR analysis, fluorescence in situ hybridization (FISH) and immunohistochemistry (IHC) data consistently supported the findings obtained by RNA-sequencing and bioinformatic analysis. While nerve injury greatly induces the *Gpr151* RNA levels, *Gpr151* protein levels are not upregulated by nerve injury but instead downregulated significantly (Figures 1E, 1F, 1G and 1H). These results showed that *Gpr151* was the most upregulated and abundant injury-responsive gene with little association to ribosome and was suitable for studying the non-coding function of a coding RAG for regulating axon regeneration. In addition to its injury responses, *Gpr151* is a single-exon gene and therefore it allows us to trace a single transcript form without considering alternatively spliced isoforms.

115 **Figure 1.**

116

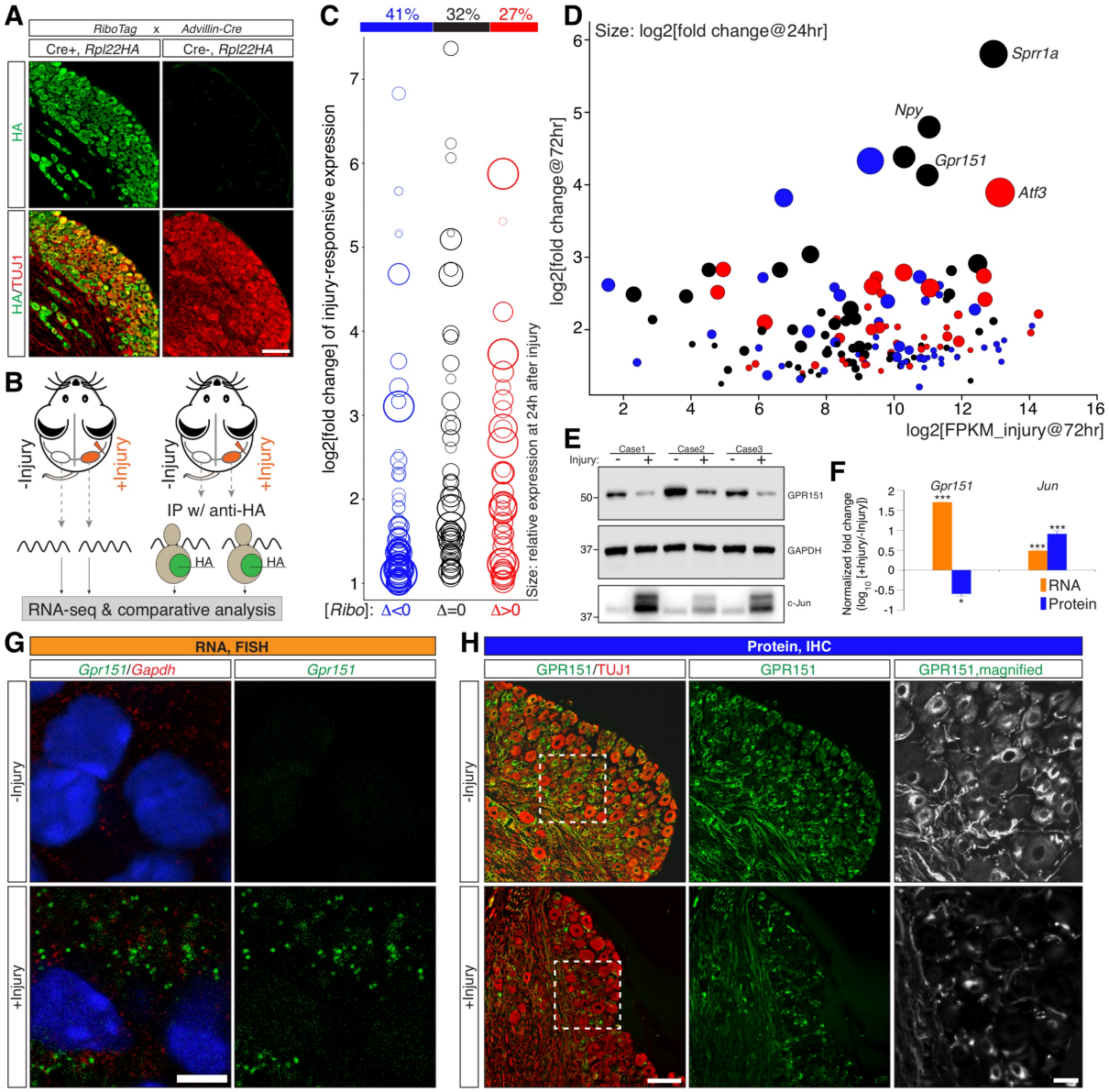

117

118

119 **Figure 1. *Gpr151* is the most upregulated and abundant injury-responsive single-exon gene**

120 **that is not directed to ribosome.** (A) *Advillin-Cre* line crossed with *RiboTag* mice expresses HA-

121 *Rpl22* specifically in DRG neurons (L4 DRG sections immunostained with anti-HA and TUJ1

122 antibodies). Scale, 100μm. (B) Comparative analysis of gene expression and the ribosome-

123 association. IP, immunoprecipitation. (C) Differential expression (Log_2 reads[@injured /

124 @uninjured]) plotted against differential ribosome-association ([*Ribo*]Δ = reads[@injured-

125 @uninjured]). The size of circle indicates the relative expression level at 24 hours after injury. (D)

126 3D plot of illumina sequencing results from the reference (Shin et al., 2019) with x-axis of
127 log_2[FPKM at 72 hours after injury] and y-axis of log_2[fold changes at 72 hours after injury]. The
128 bubble sizes indicate log2[fold changes at 24 hours]. (E) Western blot analysis of L4,5 DRG tissues
129 with or without sciatic nerve injury. (F) Relative levels of log_{10}[RNA or protein], respectively (n=3;
130 mean±SEM; *p<0.05, ***p<0.001 by *t*-test). (G) FISH analysis of L4 DRG sections with probes to
131 *Gpr151* and *Gapdh* and DAPI. Scale, 5 μm. (H) Immunohistochemistry of L4 DRG sections
132 prepared at 24 hours after sciatic nerve injury, stained with anti-GPR151 antibody (green) and
133 TUJ1 antibody (red). Scale bar, 100 μm.

134
135

136 ***Gpr151* protein-null mouse displayed no impairment of axon regeneration**

137 To investigate the role of *Gpr151* for axon regeneration, we employed *Gpr151*-targeted
138 mutant mice (KO) in which the *Gpr151* CDS was disrupted by a *LacZ* cassette to abolish *Gpr151*
139 protein production. However, the KO mice expressed mutant mRNA (*Gpr151*-UTR-*LacZ*) with the
140 wild type 5'UTR (Figure 2A). First, we tested the injury-responsive upregulation of the normal and
141 mutant *Gpr151* transcripts from the DRG tissue of the control and KO mice, respectively at 1 and
142 3 days after introducing axonal injury. We found that the levels of *Gpr151*-UTR-*LacZ* RNA from the
143 KO mice were three-fold higher than those of control *Gpr151* wild type mRNA at 1 day after injury
144 and sustained for 3 days after the injury, indicating that the KO mice were still able to express UTR
145 of Gpr151 and more immediately responding to injury than control (Figure 2B).

146 Next, the regenerative capacity was monitored by in vivo axon regeneration assays using
147 anti-SCG10 antibody (Shin et al., 2012a, 2014), showing that the KO mice exhibited enhanced
148 axon regeneration after sciatic nerve injury compared to the control mice (Figures 2C, 2D, and 2E).
149 To determine whether this enhancement is due to a neuronal effect, the regenerative potential of
150 the cultured DRG neurons from the control and KO mice was monitored under a pre-conditioning
151 injury paradigm. Without a pre-conditioning injury (-Injury), the DRG neurons cultured from both
152 the control and KO mice did not project their axons efficiently (Figure 2F). However, a pre-
153 conditioning injury (+Injury) strongly promoted axon regeneration. Notably, the DRG neurons from
154 the KO mice regenerated much longer axons than those from the control mice as seen from in vivo
155 sciatic nerve regeneration (Figures 2F, 2G and 2H). The number of DRG neurons of KO mice with
156 an axon length shorter than 100 μm was less than 50% of that of the control mice, while the KO
157 mice had two-fold more neurons with axons longer than 300 μm compared to the control (Figure
158 2I).

159 These results showed that Gpr151 protein is not required for efficient axonal regrowth
160 after injury. Instead, neurons from the protein-null mutant mice could project their axons more
161 robustly, hypothetically suggesting that the negative function of the Gpr151 protein in axon
162 regeneration. It is also possible that the KO mice displayed a more potent regenerative capacity
163 because of the more immediate upregulation of *Gpr151*-UTR-*LacZ* compared to the normal

164 *Gpr151* mRNA from the control mice 1 day after the injury (Figure 2B). *Gpr151* is an injury-
165 responsive gene that has no function of its protein for regeneration.

166 **Figure 2.**

167

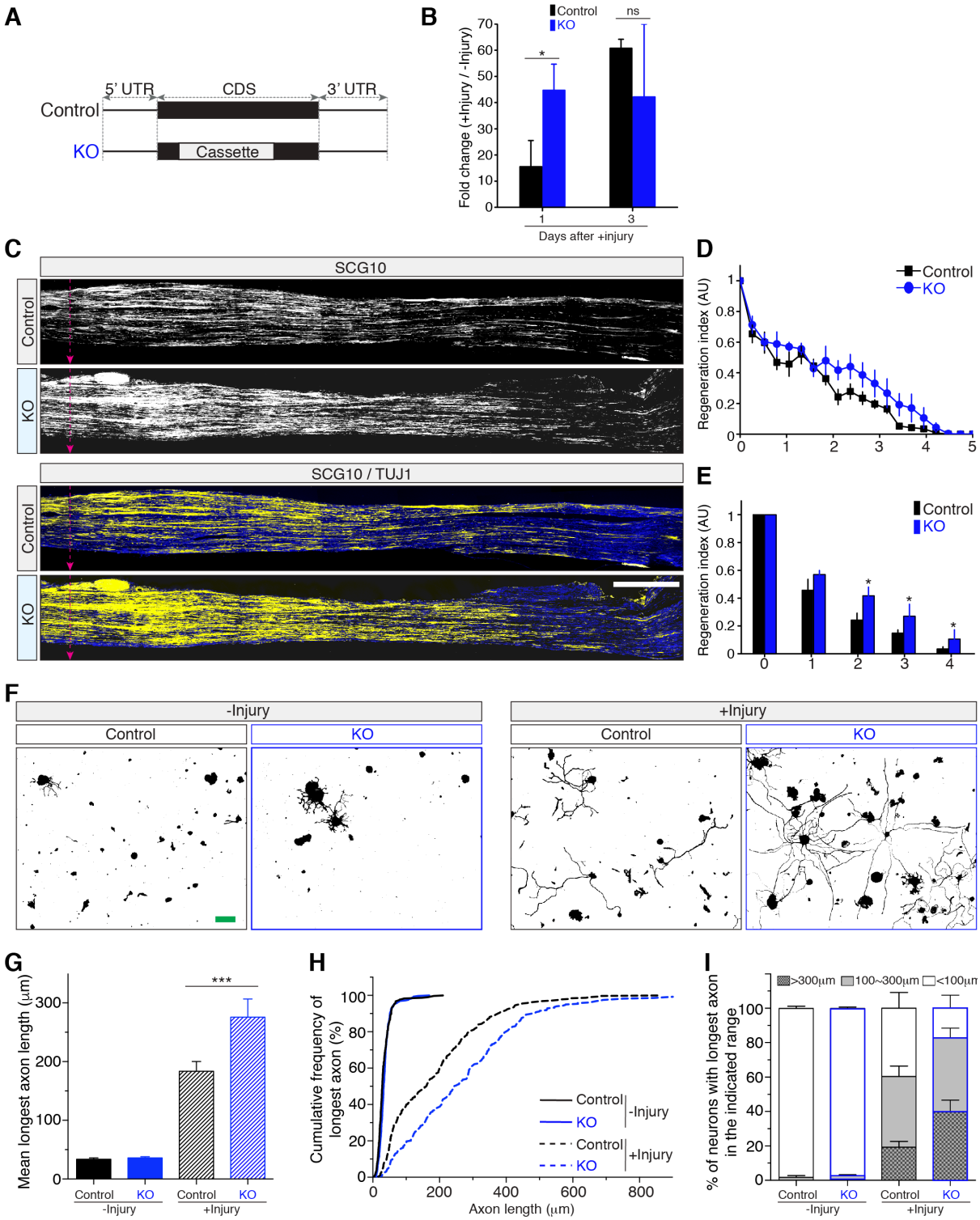

168
169

170 **Figure 2. *Gpr151* protein-null mice have no impairment of axon regeneration.** (A) Schematic

171 diagram of *Gpr151* gene in control or targeted knockout (KO) mice. (B) Average fold changes of

172 control or mutant *Gpr151* mRNA levels at 1 or 3 days after sciatic nerve axotomy (n=3 for each;

173 *p<0.05, ns, not significant, ANOVA followed by Tukey tests). (C) In vivo axon regeneration assay.
174 Sciatic nerves from control or Gpr151 protein-null mice (KO) were crushed and dissected at 3 days
175 after injury, immunostained with anti-SCG10 antibody and TUJ1 antibody. Scale bar, 500μm. (D
176 and E) Regeneration index from (C) (n=7 for control and n=5 for KO; *p<0.05 by t-test; mean±SEM).
177 (F) Adult DRG neurons cultured to monitor neuronal pre-conditioning effect. Mouse L4-5 DRG
178 tissues were dissected at 3 days after sciatic nerve axotomy (+Injury) and plated. Scale bar, 100μm.
179 (G) Average of the longest axon length from (F) (three mice for each condition, 304, 313, 291, 283
180 cells for each condition; ***p<0.001 by ANOVA followed by Tukey tests). (H) Cumulative frequency
181 of the longest axon length from (F). (I) Percentage of neurons in three categories of the longest
182 axon length.

183 **5'UTR of *Gpr151* mRNA is required for axon regeneration**

184 Because *Gpr151* KO mice still express a part of *Gpr151* mRNA including 5'UTR sequence
185 with no impairment of axon regeneration, we investigate the role of *Gpr151* mRNA not its protein for
186 axon regeneration. First, the requirement of its mRNA was monitored by knocking down *Gpr151* mRNA
187 in cultured embryonic DRG neurons and axonal regrowth was assessed. We found that knocking down
188 *Gpr151* significantly reduced neurite regrowth (Figures 3A and 3D), showing that *Gpr151* mRNA is
189 required for efficient axon regeneration. Next, two types of *Gpr151* constructs were designed to
190 investigate the role of mRNA or protein independently; CDSw, in which the 5'UTR was followed by the
191 protein-coding region (CDS) of *Gpr151*; and CDSm, which was the same as CDSw except for a
192 mutation of the start codon from AUG to AUC (Figure 3B). Western blot analysis showed that the CDSm
193 construct was inefficient in terms of producing Gpr151 protein in the DRG neurons (Figure 3C). These
194 were overexpressed in the DRG neurons in combination with the shRNA targeting endogenous *Gpr151*
195 mRNA to monitor their ability to restore the regenerative potential. First, CDSw overexpression failed to
196 recover the regenerative potential when the endogenous *Gpr151* was knocked down. In contrast,
197 overexpressing CDSm successfully restored the axon regenerative capacity (Figures 3A and 3E).
198 These results suggest that *Gpr151* mRNA and its protein regulates axon regeneration in different ways.

199 To test the hypothesis, the 5'UTR and CDS region of *Gpr151* were expressed separately to
200 monitor their ability to alter the regenerative potential (Figure 3F). The over-production of Gpr151 protein
201 via CDS not only fail to enhance axon regeneration but actually inhibited regeneration (Figures 3F and
202 3G). However, overexpressing only the 5'UTR mRNA of *Gpr151* promoted the regenerative potential,
203 indicating that the 5'UTR is sufficient for promoting regeneration and responsible for the non-coding
204 functions of *Gpr151* that are required for regeneration. (Figures 3A, 3D, 3F, and 3G). These results
205 show that *Gpr151* is required for regeneration, functioning through its 5'UTR, while the overproduction
206 of Gpr151 protein inhibits axonal regrowth in injured DRG neurons.

207 **Figure 3.**
208

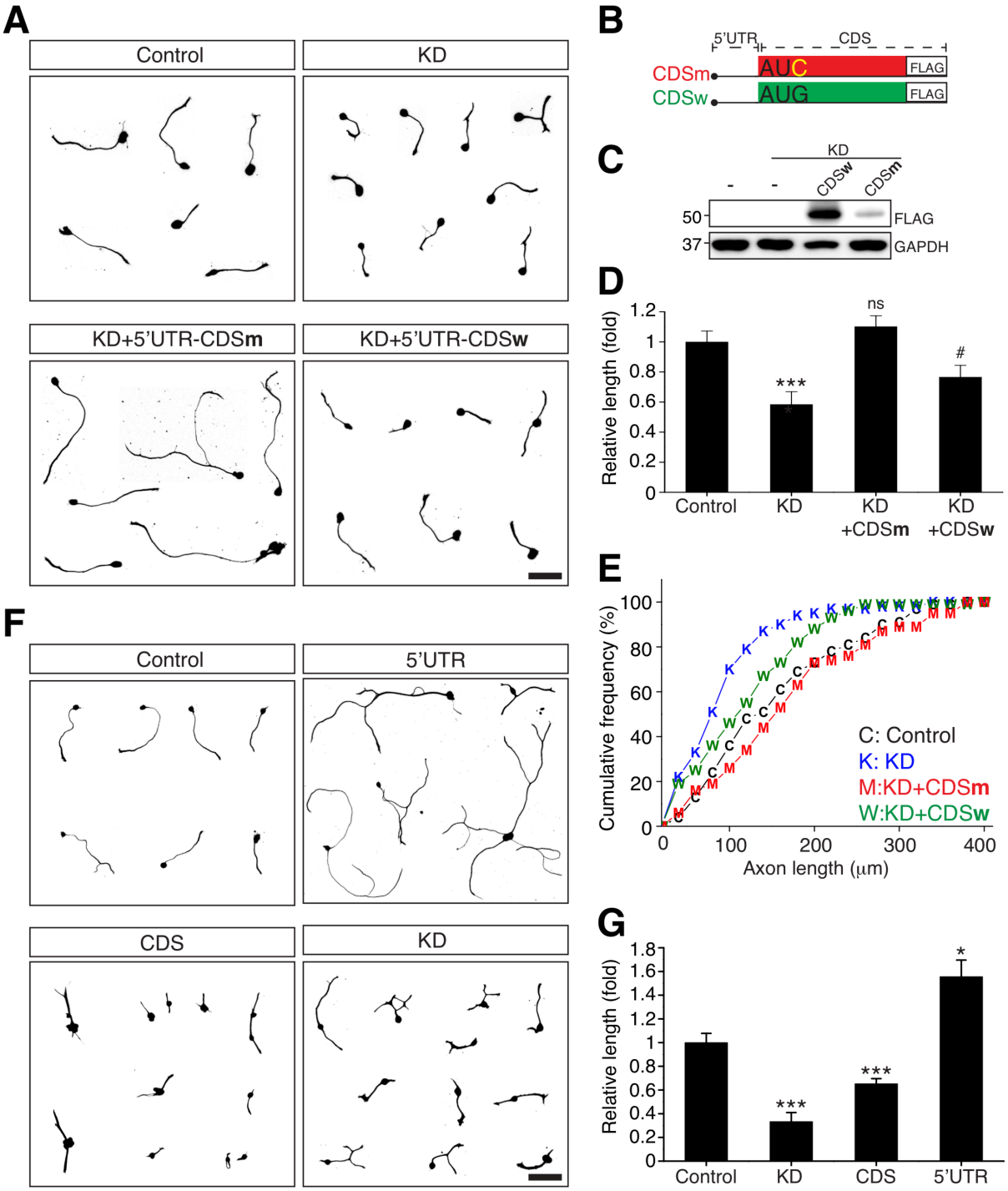

209
210

211 **Figure 3. *Gpr151* mRNA is required for axon regeneration, while its protein inhibits axonal**
212 **growth.** (A) In vitro axon regeneration assay of embryonic DRG neurons. Control, *Gpr151*-
213 knockdown (KD), *Gpr151*-knockdown (KD) with *Gpr151*-5'UTR-AUC mutant overexpression
214 (5'UTR-CDSm), and *Gpr151*-knockdown (KD) with *Gpr151*-5'UTR-AUG wild type overexpression

215 (5'UTR-CDSw). Scale bar, 100μm. (B) Schematic diagram of *Gpr151*-constructs of CDSm and
216 CDSw. AUC and AUG indicate the start codon of protein-coding sequence (CDS). 5'UTR indicates
217 5'-untranslated region of *Gpr151* gene. (C) Western blot analysis validating overexpression level
218 of the constructs CDSm and CDSw shown in (B). Anti-FLAG epitope antibody was used for western
219 blot analysis. (D) Statistical analysis of (A). Average of relative axonal length (n=67, 63, 67, 62 for
220 each condition; ***p<0.001, $^{\#}p$=0.05 by ANOVA followed by Tukey tests). (E) Cumulative frequency
221 of (A). (F) In vitro axon regeneration assay of embryonic DRG neurons. Control, 5'UTR of *Gpr151*
222 overexpression (5'UTR), protein-coding sequence overexpression (CDS), and *Gpr151*-knockdown
223 (KD). (G) Statistical analysis of (F). Average of relative axonal length (n=160, 147, 267, 161 cells
224 for each condition; *p<0.05, ***p<0.001 by ANOVA followed by Tukey tests).

225 **The 5'UTR of *Gpr151* binds to CSDE1, a negative regulator of axon regeneration**

226 To understand the molecular mechanisms underlying the role of *Gpr151*-5'UTR, RNA pull-
227 down assays and mass spectrophotometry analysis were conducted to identify the 5'UTR of
228 *Gpr151* mRNA-interacting proteins. A total of 25 proteins were identified with high confidence
229 scores and matched masses (Figure 4A and Supplementary information 1). Among them, we
230 determined to investigate the involvement of CSDE1 because of its known neuronal roles. First,
231 CSDE1 is a negative regulator of neural differentiation in human stem cells because loss of CSDE1
232 accelerates neurogenesis (Ju Lee et al., 2017). Second, likely gene-disrupting variants in CSDE1
233 are associated with autism spectrum disorder (Guo et al., 2019). Interestingly, it was reported that
234 CSDE1 knockdown promotes neurite and axon outgrowth (Guo et al., 2019). These results
235 stimulated us to hypothesize that CSDE1 is a key target of *Gpr151* mRNA for its non-coding
236 function through non-ribosomal RBPs. Furthermore, we found the existence of the CSDE1-binding
237 motif sequences that are evolutionary conserved among the 5'UTR of mouse, rat and human
238 *GPR151* mRNA at upstream of start codon (Ju Lee et al., 2017; Moore et al., 2018; Saltel et al.,
239 2017) (Figure 4B).

240 The interaction between the 5'UTR and CSDE1 was confirmed by RNA pull-down assays
241 using biotinylated 5'UTR as a bait, followed by western blot analysis using an anti-CSDE1 antibody
242 (Figure 4C). The interaction was reversely verified using immunoprecipitation of CSDE1 in DRG
243 tissue lysates. CSDE1 was immunoprecipitated and subjected to RT-qPCR analysis for *Gpr151* to
244 confirm that *Gpr151* mRNA upregulated by nerve injury was strongly associated with CSDE1
245 (Figure 4D). The sharp increase in the CSDE1-associated *Gpr151* mRNA shows a clear contrast
246 to its affinity to ribosome complexes, which was unchanged after injury (Figure 1). To determine if
247 the CAAGAA sequence in the 5'UTR was responsible for the interaction with CSDE1, a CAAGAA-
248 deleted mutant (ΔCSDE1) and artificial 32-mer RNA with only a 4X-repeated A-CAAGAA-G
249 sequence (4X) was subjected to RNA pull-down assays (Figure 4E). The following western blot
250 analysis showed that the artificial RNA 4X had a stable association with CSDE1, whereas the
251 interaction of ΔCSDE1 was significantly destabilized (Figure 4F). Human *GPR151* mRNA also has
252 the CSDE1-binding motif in the 5'UTR, and the interaction between CSDE1 and the 5'UTR of

253 *GPR151* was also confirmed (Figure 4G). These results indicated that the CAAGAA sequence in
254 the 5'UTR of *Gpr151* is primarily responsible for binding to CSDE1.

255 Although CSDE1 is known to function in neurons (Guo et al., 2019; Ju Lee et al., 2017),
256 there is no evidence showing that CSDE1 plays a role in axon regeneration. Therefore, we
257 investigate the role of CSDE1 in an axon injury model by in vitro axon regeneration assays from
258 embryonic DRG neurons. We found that the regenerative potential of the neurons was promoted
259 by around 50% when CSDE1 was knocked down (Figures 4H and 4I). The RBP KHDRBS1 that
260 was also identified as a binding protein of *Gpr151*-5'UTR was also knocked down for testing its
261 involvement in axon regeneration but had no effect on axon regeneration, supporting a specific
262 function of CSDE1. This suggests that CSDE1 has a potential function as a negative regulator of
263 axon regeneration, implying that the 5'UTR of *Gpr151* might interact to modulate the function of
264 CSDE1 in regeneration.

265 CSDE1 is known to bind to single-stranded RNA, regulating mRNA translation
266 (Triqueneaux et al., 1999; Wurth et al., 2016). The prediction of the RNA secondary structure of
267 the 5'UTR indicated that the CSDE1-binding motif in the 5'UTR of *Gpr151* is partially single-
268 stranded (colored letters in 5'UTR$_{WT}$, Figure 4J). To explore the possibilities for manipulating the
269 5'UTR-CSDE1 interaction and engineering the 5'UTR for potential applications, we generated
270 three mutant 5'UTR forms: 1) h, the shortest 11-mer RNA without a CSDE1-binding motif; 2)
271 5'UTRm, the full 5'UTR sequence but with the AGCUU at the -5 bp substituted with the
272 complementary sequence UCGAA so that the binding motif CAAGAA became fully single-stranded;
273 and 3) Δ, the 5'-part of the 5'UTR including the CSDE1-binding motif but no stem-loop region
274 (Figure 4J). We found that h did not bind to CSDE1, confirming the previous results obtained using
275 ΔCSDE1 (Figure 4F). However, 5'UTRm and Δ both displayed a more stable association than did
276 5'UTR$_{WT}$ (Figure 4K), suggesting that the CAAGAA sequence in the 5'UTR is required for its
277 association with CSDE1 and that the interaction is stabilized when CAAGAA is single-stranded.
278 Following this, Δ was used as a molecular competitor for bait-competition pull-down assays
279 (Figures 4L and 4M). The competition assays revealed that the interaction between the 5'UTR and
280 CSDE1 was impaired when the concentration of the competitor was increased for both mouse

281 *Gpr151* and human *GPR151* (Figures 4L and 4M). Overall, our biochemical analysis confirmed
282 that CSDE1 is the biological interactor for *Gpr151* mRNA and that the 5'UTR of *Gpr151* mRNA is
283 responsible for this interaction.
284

285 **Figure 4.**

286

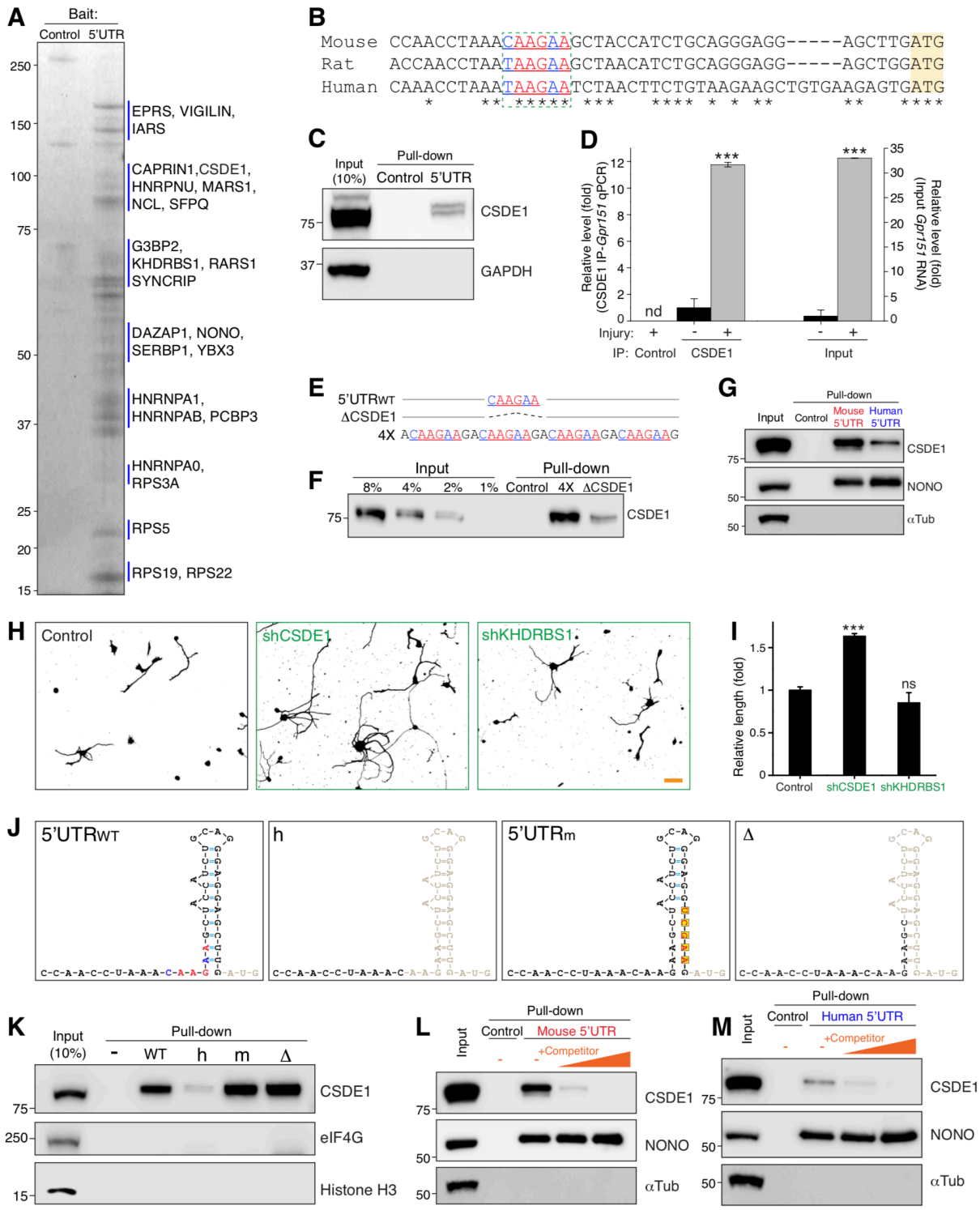

287

288

289 **Figure 4. CSDE1 is a negative regulator of axon regeneration interacting with 5'UTR of**

290 ***Gpr151* mRNA.** (A) Coomassie staining of SDS-PAGE of 5'UTR-binding proteins. (B) Alignment

291 of 5'UTR sequences of mouse, rat and human *GPR151* gene. Green box, nAAGnA, CSDE1-

292 binding consensus motif, yellow shadow, the start codon of *Gpr151* CDS. (C) Western blot analysis

293 of 5'UTR pull-down assay. (D) Relative folds of *Gpr151* mRNA levels analyzed by RT-qPCR (n=3,
294 ***p<0.001, nd, not determined by t-test; mean±SEM). (E) Illustration of the artificial RNA
295 sequences of ΔCSDE1 or 4X mutant. (F) Western blot analysis of pull-down assay with the baits,
296 ΔCSDE1 or 4X mutant. (G) Western blot analysis of pull-down assay with the baits, mouse 5'UTR
297 or human 5'UTR of *GPR151*. (H) In vitro axon regeneration assay from control, CSDE1 knockdown
298 (shCSDE1) and KHDRBS1 knockdown (shKHDRBS1) embryonic DRG neurons. Scale bar,
299 100μm. (I) Statistical analysis of regenerating axon length of (H) (n=254, 198, 167 for control,
300 shCSDE1 and shKHDRBS1; ***p<0.001, ns, not significant by ANOVA followed by Tukey tests;
301 mean±SEM). (J) Illustrations of the secondary structures of 5'UTR of *Gpr151* wild type ($5'UTR_{WT}$),
302 no CSDE1-binding motif (h), single-stranded CSDE1-binding motif (5'UTRm) and no stem (Δ)
303 mutant. (K) Western blot analysis of pull-down assay with the baits of (J). (L and M) Western blot
304 analysis of pull-down assay with the competitor Δ for mouse and human 5'UTR.

305 **5'UTR of *Gpr151* modulates the CSDE1-associated RNA pool to promote axon regeneration**

306 Because CSDE1 functions as a negative regulator of axon regeneration in vitro (Figures 4H
307 and 4I), we next tested whether this function is modulated by its interaction with the *Gpr151*-5'UTR.
308 First, we compared the regenerative potential of 5'UTR$_{WT}$ and 5'UTRm-overexpressing neurons to
309 determine whether the enhanced CSDE1-binding affinity of 5'UTRm affects its ability to promote
310 axon regeneration. We found that 5'UTR$_{WT}$ promoted axon regeneration by up to 50% compared
311 to the control (Figures 5A and 5B), consistent with the results of the initial assay (Figure 2G).
312 However, 5'UTRm expression led to significantly more robust regeneration than did 5'UTR$_{WT}$
313 expression (Figures 5A and 5B). To verify that the enhanced function of 5'UTRm requires the
314 association with CSDE1, an additional mutation deleting the CSDE1-binding motif was introduced
315 to 5'UTRm (5'UTRm∆CSDE1) and was tested for its effect on regeneration. We found that the
316 mutant 5'UTRm∆CSDE1 did not promote axon regeneration as much as 5'UTR$_{WT}$ did (Figure S3),
317 suggesting that the function of 5'UTR in regeneration is dependent on its physical association with
318 CSDE1.

319 As 5'UTRm effectively enhances axon regeneration, we used the mutant 5'UTRm for
320 studying the mechanisms involved in the regulation of CSDE1 by 5'UTR. Based on the known role
321 of CSDE1 as an RBP regulating the interacting mRNA, we hypothesized that 5'UTRm, by binding
322 to CSDE1, may induce dissociation of the interacting mRNA and inhibit the function of CSDE1.
323 We developed a comparative analysis for 5'UTR-induced changes in CSDE1-associated mRNA,
324 one similar to the initial analysis for *Rpl22*-HA IP-seq in Figure 1B, and also assessed 5'UTRm-
325 dependent DEGs to control for the mRNA levels. Notably, a group of mRNAs (19.0% of total)
326 exhibited significant changes in their binding behavior with CSDE1 following 5'UTRm
327 overexpression without corresponding changes in their expression levels (78.6%, $-1 < \mathrm{Log}_2$[Fold
328 change] < 1). A large number among these mRNA (16.9% of total) were dissociated from CSDE1,
329 while a smaller group (2.7%) formed a more stable association (Figure 5C and Supplementary
330 information S2). Meanwhile, the majority of the mRNAs (80.4%) did not demonstrate dramatic
331 changes in their interaction with CSDE1, even when they were differentially expressed (8.4%).
332 Additionally, there were DEGs with mRNA that was up- (11.6%) or downregulated (9.9%) over

333 two-fold (Figure 5C). The comparative analysis revealed that 5'UTRm overexpression regulated
334 the pool of CSDE1-associated coding mRNAs, suggesting that the dissociation of these mRNA is
335 responsible for the CSDE1-dependent function of *Gpr151*-5'UTR. These results suggest that
336 regulation of RBP function and its interaction with target mRNA can be important molecular
337 mechanisms when an mRNA appears to have a non-coding function via interaction with a specific
338 RBP.

339 Because the biological outcome of 5'UTRm is an improvement in the regenerative potential
340 under an axon injury paradigm, we investigated the biological functions of the mRNAs that are
341 released from CSDE1 after 5'UTRm overexpression. DAVID tools were utilized for gene ontology
342 and signaling pathway analysis (Dennis et al., 2003; Hosack et al., 2003; Huang et al., 2009;
343 Sherman et al., 2007). it was found that the known functions of the identified genes were
344 specifically related to regulating protein localization and transport, while cytoskeletal remodeling,
345 apoptosis, cell growth, and behavioral control functions were also enriched (Figure 5D and
346 supplementary information S3). In addition, pathway analysis revealed that genes related to
347 ribosomes and ribosome synthesis made up a significant proportion of the group of genes
348 observed to be released from CSDE1 after 5'UTRm overexpression (Figure 5E and
349 Supplementary information S4). Genes related to neurodegenerative disorders such as
350 Alzheimer's disease, Huntington's disease, Parkinson's disease, and amyotrophic lateral sclerosis
351 and to neurotrophin signaling or axon guidance were also enriched among the genes dissociated
352 from CSDE1 (Figure 5E and Supplementary information S4). This analysis shows that our
353 unconventional experimental design investigating the CSDE1-interactome reveals the biological
354 pathways that have not been identified in previous DEG studies related to peripheral nerve injury
355 (Ma and Willis, 2015; Shin et al., 2018, 2019). The genes identified in these pathways also did not
356 exhibit any significant changes in their expression levels, suggesting that a simple DEG analysis
357 may not pick them up.

358 Finally, we analyzed proteomic changes in control and 5'UTRm-overexpressing neurons.
359 Antibody-array analysis showed that 5'UTRm induced the differential up- (14.9%) or
360 downregulation (17.4%) of a total of 1,358 target proteins (Figure 5F and Supplementary

361 information S5). We subjected these to a comparative analysis with CSDE1 IP-seq data and found
362 that the mRNAs encoding the target proteins exhibited distinctive changes in their CSDE1-
363 associated conditions after 5'UTRm overexpression (Figure 5G and Supplementary information
364 S6). A group of mRNAs, including *Eef1g*, *Fgfr2*, and *Scng* (red-closed circles, 0.8%), were
365 dissociated from CSDE1 when 5'UTRm was overexpressed (Figure 5G and Supplementary
366 information S6). However, a large number of mRNAs, including *Ywhaz* (open circles), had no
367 significant changes in their protein levels, while another group that were released from CSDE1
368 (e.g., *Tshz2*, *Tubb3*, *Mta1*, and *Nr2f2l*) experienced a reduction in their protein levels. This
369 suggests that the mRNAs released from CSDE1 have different fates in terms of their routes to
370 either ribosomes or other RBPs when promoting the regeneration of neurons.
371

372 **Figure 5.**

373

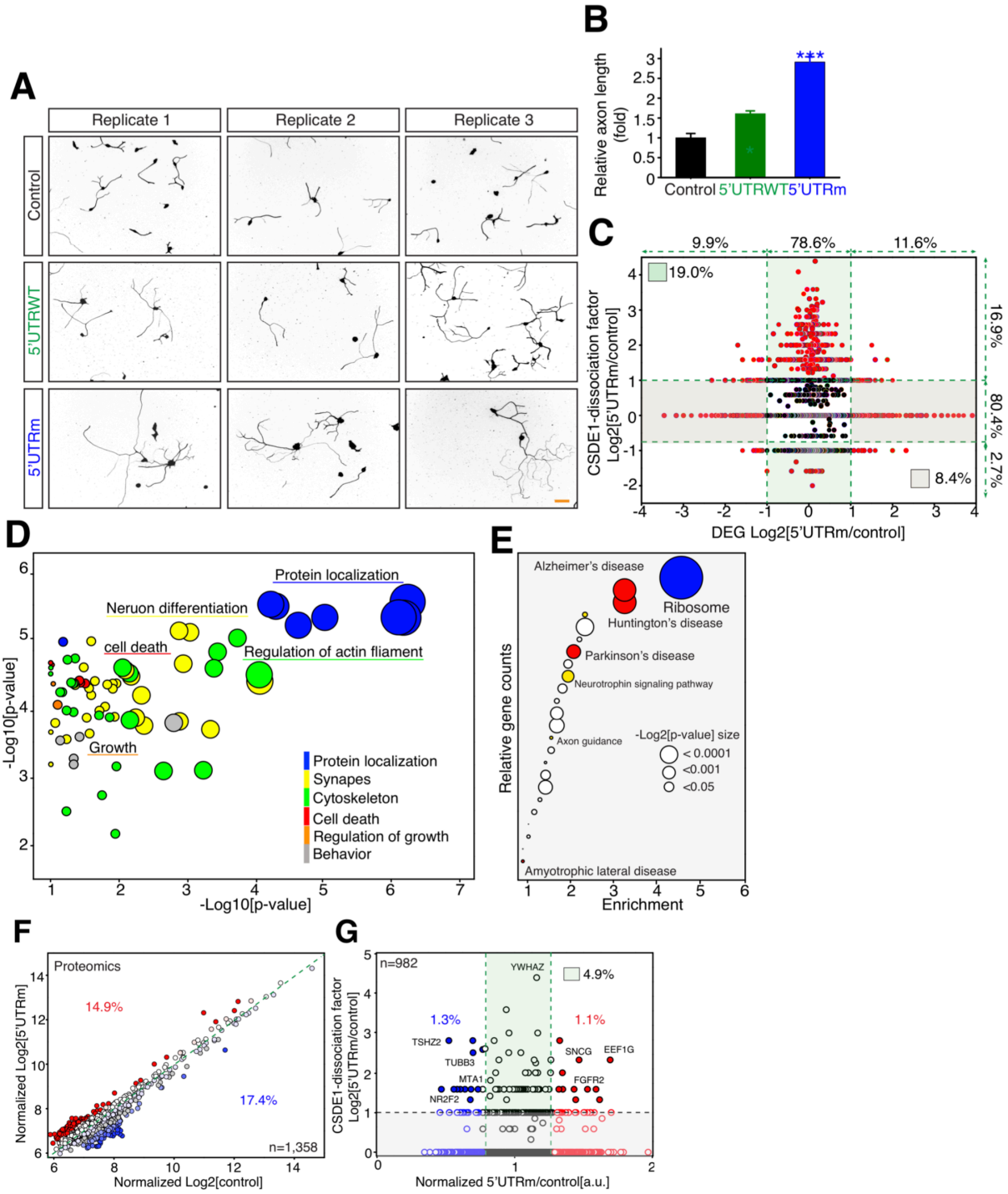

374

375

376 **Figure 5. Expressing engineered 5'UTR of *Gpr151* mRNA modulates CSDE1-RNA interaction,**

377 **resulting in dissociation of an RNA group related to distinct biological processes.** (A) In vitro

378 axon regeneration assay of embryonic DRG neurons expressing control vector, 5'UTR of *Gpr151*

379 (5'UTR$_{WT}$) or a mutant 5'UTR with single-stranded CSDE1-binding motif (5'UTRm). Scale bar,
380 100μm. (B) Statistical analysis of relative average axon length from (A) (n=97, 104, 98 cells for
381 control, 5'UTR$_{WT}$ and 5'UTRm; *p<0.05, ***p<0.001 by ANOVA followed by Tukey tests;
382 mean±SEM). (C) Two-dimensional plot with the x-axis of log2-transformed fold changes of
383 [reads@5'UTRm / reads@control] and the y-axis of. See also supplementary information S2. (D
384 and E) Gene ontology analysis (D) and KEGG pathway analysis (E) of the genes dissociated from
385 CSDE1 by 5'UTRm overexpression, shown in the upper green box in (C). (F) Proteomic analysis
386 of antibody array results with the x-axis of normalized log2-transformed values in control and y-
387 axis of normalized log2-transformed values in 5'UTRm. The color red and blue indicates
388 upregulated or downregulated target protein by 30% or more, respectively. Percentages indicate
389 the relative ratios of the colored targets of total 1,358 probes. (G) Target proteins in (F) are plotted
390 for the corresponding CSDE1-dissociation factor of their mRNA, negative log2-transformed fold
391 changes of CSDE1-IP [reads@5'UTRm / reads@control].

392 **Expression of the engineered RNA promotes axon regeneration in vivo**

393 To test if the engineered 5'UTR of *Gpr151* is a potential tool for promoting the regenerative
394 capacity in vivo, adeno-associated virus (AAV) expressing 5'UTRm was utilized for in vivo gene
395 delivery in two different axon regeneration models. In PNS axon regeneration assays, mouse
396 sciatic nerves were damaged via crush injury and dissected 3 days after the injury (Figure 6A).
397 The sciatic nerves of 5'UTRm-expressing mice exhibited a dramatic increase in their axon
398 regeneration as observed in the regeneration assays using cultured neurons (Figures 6B, 6C and
399 6D). Similar results were reproduced in central nervous system (CNS) axon regeneration assays
400 with an optic nerve injury model (Figure 6F). The regenerating axons in the optic nerves were
401 traced using cholera toxin B (CTB). We found that 5'UTRm overexpression dramatically increased
402 the number of regenerating axons in the injured optic nerves (Figures 6F and 6G).

403 The neuronal injury responses in the PNS and the CNS are known to be differentially
404 regulated, resulting in significantly inefficient axon regeneration in the CNS compared to that in the
405 PNS (Curcio and Bradke, 2018; He and Jin, 2016; Mahar and Cavalli, 2018). Hence, to test if the
406 marked upregulation of *Gpr151* is a molecular response specific to the PNS, where regeneration
407 is robust, qPCR for *Gpr151* was performed in both systems. *Gpr151* mRNA is upregulated in the
408 DRG neurons after sciatic nerve injury, while it was not observed in the retinal tissue after optic
409 nerve injury (Figure 6H). This suggests that the PNS and the CNS may have different injury-
410 responsive epigenetic mechanisms regulating *Gpr151* expression (Jiang et al., 2018). However,
411 both systems produced similar outcomes in the promotion of axon regeneration when the *Gpr151*-
412 5'UTRm was overexpressed. Therefore, components in the downstream signal transduction
413 regulated by 5'UTR may be available to function in both systems.

414

415 **Figure 6.**

416

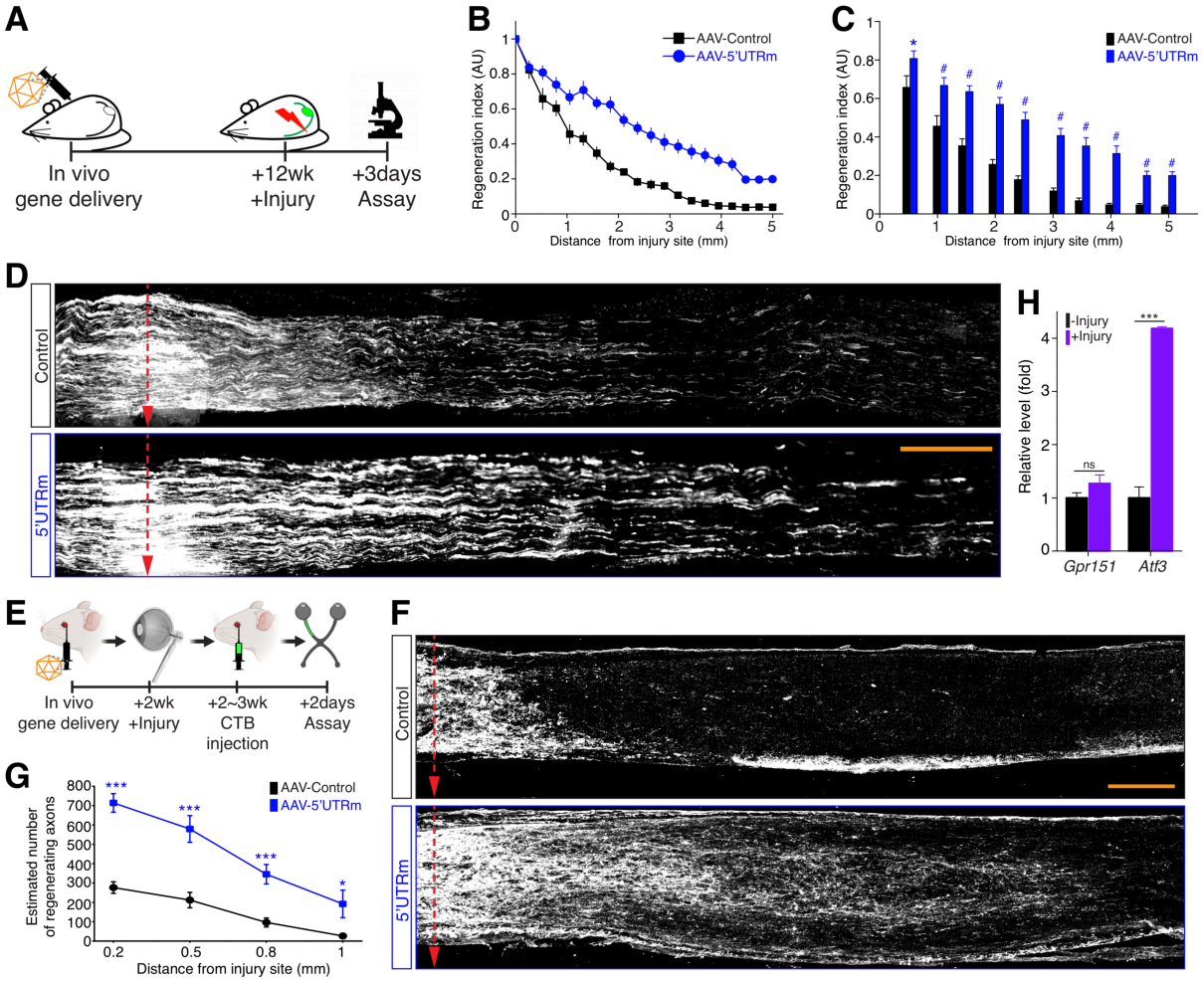

417

418

419 **Figure 6. In vivo gene delivery of engineered 5'UTR of *Gpr151* mRNA promotes axon**

420 **regeneration.** (A) Experimental scheme of in vivo gene delivery for in vivo axon regeneration

421 assay in mouse sciatic nerves (wk, week(s)). (B and C) In vivo regeneration index from (D) (n=8

422 for control, 10 for 5'UTRm; *p<0.05, $^{\#}p$<0.001 by t-test; mean±SEM). (D) In vivo axon regeneration

423 assay from sciatic nerves. Representative longitudinal sections of the sciatic nerves from control

424 or 5'UTRm-expressing mice. Red dotted arrows indicate the injury site. Scale bar, 500μm. (E)

425 Experimental scheme of in vivo gene delivery for in vivo axon regeneration assay in mouse optic

426 nerves (wk, week(s)). (F) Representative longitudinal sections of optic nerves from control or

427 5'UTRm-expressing mice. Red dotted arrows indicate the injury site. Scale bar, 200μm. (G)

428 Estimated numbers of regenerating axons (n=5 for control, 6 for 5'UTRm; *p<0.05, ***p<0.001 by

429 t-test; mean±SEM). (H) qPCR analysis of *Gpr151* and *Atf3* from mouse retina with (+Injury) or
430 without (-Injury) injury (n=3 for each condition; ***p<0.001, ns, not significant by t-test; mean±SEM).
431

432 **Retrospective analysis shows that *Sox11* regulates the regenerative potential via 5'UTR**

433 We were motivated to re-analyze our previously published injury-responsive
434 transcriptomic data to search for additional examples of injury-induced mRNA with potential non-
435 coding function. Dual leucine zipper kinase (DLK) is a key molecule regulating injury responses
436 including axon regeneration and degeneration and it is required for the regenerative transcriptional
437 program by activating a mitogen-activated protein kinase (MAPK) pathway (Shin et al., 2012b).
438 Previously, we identified injury-responsive DLK-dependent transcriptome in a sciatic nerve
439 regeneration model at different time points after injury (Shin et al., 2019a). We re-plotted these
440 original gene expression profiles to show the relationship between DLK dependency and injury
441 responsiveness, with the size of the circles indicating the relative fold change 72 hours after injury
442 (Figure 7A). The individual genes are colored according to their ribosome-association efficiency
443 as identified in the present study (Figure 1C). We found that only 21% of the 593 DLK-dependent,
444 injury-responsive upregulated genes exhibited an increase in their ribosome-association efficiency
445 (red circles, Figure 7A), consistent with the results shown in Figure 1C. To test the highly DLK-
446 dependent and injury-responsive mRNA group for the potential non-coding function, we again
447 selected single-exon genes. *Jun*, *Sox11*, and *Ier5* comprised the single-exon gene group with DLK-
448 dependent upregulation after injury. *Jun* and *Sox11* displayed increased ribosome-association
449 after nerve injury (red circle) whereas the ribosome-association of *Ier5* mRNA was unchanged
450 (gray circle) (Figure 7A). These genes were subjected to in vitro axon regeneration assays to
451 investigate the requirements for regeneration. Of the three candidate genes, *Sox11* was found to
452 be required for axon regeneration (Figures 7B and S4). *Sox11* encodes a transcription factor that
453 has been implicated in the regulation of axon regeneration (Jankowski et al., 2018; Li et al., 2018;
454 Norsworthy et al., 2017). We tested whether *Sox11* mRNA plays a non-coding function via its UTR,
455 similarly to the case of *Gpr151*. We found that *Sox11* knock-down reduced the regenerative
456 potential, but *Sox11*-knockdown neurons recovered their regenerative capacity when the 5'UTR of

457 *Sox11* mRNA was overexpressed (Figures 7B and 7C). These results demonstrate that *Sox11* is
458 required for axon regeneration and that the 5'UTR of *Sox11* mRNA is sufficient for positively
459 regulating the regeneration process through a non-coding function. Because *Sox11* mRNA
460 became more strongly associated with ribosome complexes when *Sox11* mRNA was upregulated
461 after axonal injury, Sox11 protein may also have a specific role in regulating axon regeneration,
462 independent of the non-coding function of its mRNA. Collectively, our approach to investigate
463 single-exon genes for their translation-independent mRNA function uncovers an additional
464 example of injury-induced coding and non-coding RNA (cncRNA), *Sox11* mRNA, that promotes
465 axon regeneration after injury.

466 Taken together, our data demonstrate the non-coding function of *Gpr151* mRNA for
467 promoting axon regeneration via the association of its 5'UTR with CSDE1 and suggest the need
468 for the separate functional tests of mRNA and its protein in DEG studies to understand the
469 mechanisms underlying cellular responses.
470

471 **Figure 7.**
472

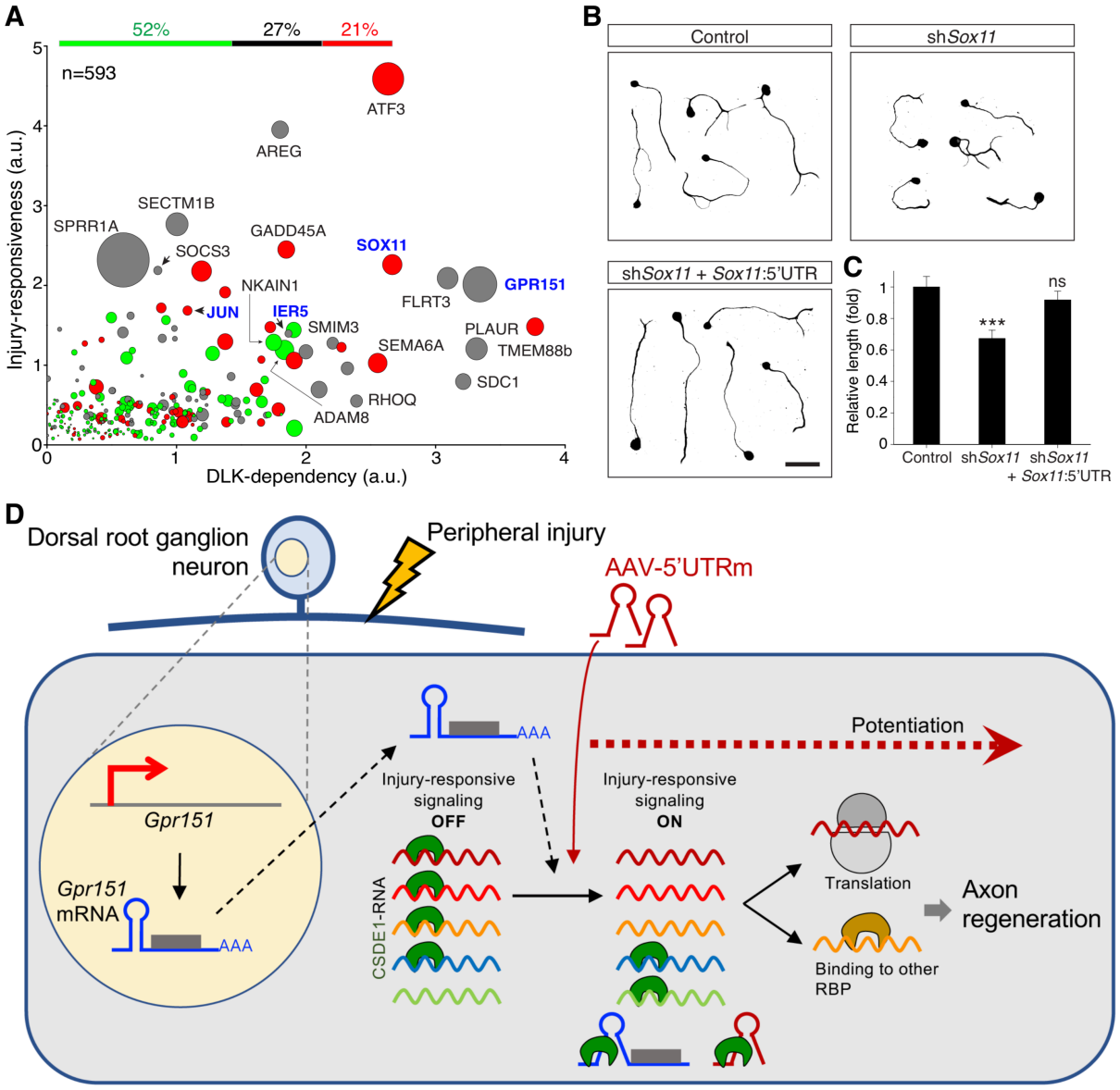

473
474
475 **Figure 7. Retrospective re-analysis of the previously published DEG data suggests 5'UTR**
476 **of *Sox11* regulates neuronal potential for axon regeneration.** (A) Three-dimensional plot with
477 the x-axis of DLK-dependency (a.u.), the y-axis of injury-responsiveness (a.u.) and the circle
478 sizes of the relative fold change at 72 hours after injury. The colors indicate ribosome-association
479 efficiency; red, increased, black, not changed and green, decreased at 24 hours after injury. Total
480 593 genes were selected as DLK-dependent injury-responsive genes. (B) In vitro axon
481 regeneration assay of re-plated embryonic DRG neurons. Control, *Sox11* knock-down (sh*Sox11*)
482 and *Sox11* knock-down with 5'UTR of *Sox11* overexpression (sh*Sox11* + *Sox11*:5'UTR). Scale
483 bar, 100 μm. (C) Average relative axon length of (C) (n=63, 86, 70 cells for each; ***p<0.001, ns,

484 not significant by ANOVA followed by Tukey tests; mean±SEM). (D) Illustration of the proposed

485 model.

486

487 **Discussion**

488 Neuronal responses after injury have been investigated using various experimental tools
489 to identify important mechanisms regulating the neuron-intrinsic regeneration program (Curcio and
490 Bradke, 2018; Dulin et al., 2015; He and Jin, 2016; Ma and Willis, 2015). Emerging omics
491 technologies have facilitated the gaining of new knowledge in the axonal regeneration pathway
492 (Tedeschi and Popovich, 2019). For example, DEG analysis is often used as a method to identify
493 genes regulating the neuronal injury responses, based on the premise that significantly
494 upregulated or downregulated genes may be functionally important for the biological process.
495 Indeed, transcriptome studies in injured peripheral neurons have uncovered injury-responsive
496 genes, among which a subset has been implicated in the regulation of axon regeneration. However,
497 there still remain many injury-induced genes without clearly defined function in axonal regeneration
498 or other injury responses. To overcome the limitation of single-omics approach and enhance
499 selectivity for interesting features of genes, we took multi-omics combinatorial methods. There
500 were earlier studies taking combinatorial approach comparing injury-induced proteome and
501 transcriptome to identify signaling networks that are required for activation of the transcriptional
502 regenerative program (Kong et al., 2020; Michaelevski et al., 2010; Tedeschi and Popovich, 2019).
503 In the present study, we compared transcriptome and ribosome-association efficiency of protein-
504 coding DEGs after sciatic nerve injury to directly address the fates of the injury-responsive mRNA.
505 We identified a group of genes that are upregulated in response to axonal injury without changes
506 in their ribosome-association efficiency, supporting a striking discordance between transcriptional
507 and translational controls after injury.

508 *Gpr151* was one of the injury-responsive genes whose dramatic upregulation after nerve
509 injury has consistently been reported in several DEG studies (Förstner et al., 2018; Holmes et al.,
510 2017; Jiang et al., 2015, 2018; Reinhold et al., 2015; Shin et al., 2019; Stern et al., 2012; Tedeschi
511 et al., 2017; Wlaschin et al., 2018). Gpr151 protein is known to play a molecular role as an orphan
512 GPCR in signaling pathways controlling addiction and pain (Antolin-fontes et al., 2019; Antolin-
513 Fontes et al., 2020; Boulos et al., 2017; Broms et al., 2015, 2017; Le Foll and French, 2018; Gorlich
514 et al., 2013; Holmes et al., 2017; Jiang et al., 2018; Stein et al., 2016). Therefore, an easily driven

515 hypothesis would be that the GPCR function of Gpr151 is enhanced by the increased gene
516 expression and contributes to the regulation of the regenerative signaling after injury. However, in
517 contrast to this notion, we found that the upregulated *Gpr151* mRNA is not directed to ribosome
518 complexes from our *RiboTag*-sequencing analysis. Instead of being associated with ribosomes,
519 upregulated *Gpr151* mRNA was associated with RBPs such as CSDE1. We found that *Gpr151*
520 mRNA binds to CSDE1 through a consensus binding sequence conserved in rodent and human
521 genes in its 5'UTR and functions as a non-coding RNA that modulates CSDE1-binding mRNA.

522 Gpr151 protein levels displayed no increase in mouse DRG tissue when axonal injury was
523 introduced. Instead, the protein levels showed a significant reduction after injury, indicating
524 additional mechanisms for regulating the Gpr151 protein levels. In addition, Gpr151 protein may
525 have a negative role in axonal growth because over-producing Gpr151 protein inhibited axon
526 regeneration in vitro. The enhanced axon regeneration observed in the sciatic nerves of the
527 *Gpr151* protein-null mutant mice also supports the inhibitory function of the Gpr151 protein. A
528 recent study by Antolin-Fontes and colleagues have demonstrated that Gpr151 interacts with the
529 G-alpha inhibitory subunit Gαo1 in habenular neurons and that their interaction inhibits adenylyl
530 cyclase, leading to a reduction in the cyclic AMP (cAMP) levels (Antolin-Fontes et al., 2020). Since
531 cAMP levels and the downstream PKA pathway are major components in the intrinsic axon
532 regeneration program, Gpr151 protein-dependent signaling may play the putative inhibitory role by
533 suppressing the cAMP-PKA pathway in regenerating peripheral neurons. Furthermore, we
534 speculate that the reduced Gpr151 protein levels observed after nerve injury might be an adaptive
535 response in the DRG neurons to circumvent the inhibitory effect of the Gpr151 pathway. The role
536 of Gpr151 protein in axon regeneration and other injury responses would be an interesting topic in
537 future studies.

538 RBPs are implicated in diverse events in the nervous system such as neurodevelopment
539 and memory consolidation and also involved in the pathogenesis of neurodegenerative diseases
540 (Conlon and Manley, 2017; Gopal et al., 2017; Hörnberg and Holt, 2013; Nussbacher et al., 2015).
541 While the main role of RBPs is to regulate the fate of interacting RNA, the functions of RBPs are
542 conversely modulated by interacting with specific regulatory RNAs (Hentze et al., 2018). Hence,

543 the molecular networks of transcripts and their interacting RBPs need to be delineated in order to
544 correctly understand functional outcome of transcriptomic changes in a specific cellular response.
545 Although we focused on CSDE1 as an interacting RBP of *Gpr151*-5'UTR, there were other RBPs
546 identified in the mass analysis that putatively interact with the 5'UTR. For example, the interaction
547 of the 5'UTR with NonO was confirmed by pull-down assays where the binding affinity was
548 unaffected by the competitor containing the CSDE1-specific binding sequence in *Gpr151*-5'UTR.
549 Therefore, it appears that NonO recognizes different sequence or structure of the 5'UTR from that
550 interacting with CSDE1. Although it is unclear whether the interaction with NonO and other RBPs
551 has regulatory roles, we suggest that CSDE1 is a major functional target of *Gpr151*-5'UTR in axon
552 regeneration because the ability of the 5'UTR to promote regeneration is aborted by deleting the
553 CSDE1-binding motif.

554 Evidence builds for mRNA functioning as cncRNA with both protein-dependent and
555 independent roles, although the role in axon-injury signaling has not been reported (Kumari and
556 Sampath, 2015; Sampath and Ephrussi, 2016). In the present study, we identified *Gpr151* as a
557 new cncRNA in the axon regeneration pathway, based on the observation that its mRNA
558 expression and ribosome-association is greatly uncoupled. As there were many other injury-
559 responsive DEGs with the disconnected ribosomal targeting, more genes might be identified as
560 cncRNA involved in the regenerative response. Likewise, our understandings of the DEG functions
561 in other cellular responses may be broadened by examining the potential non-coding roles of their
562 mRNA as regulators of the interacting RBPs. In addition, we suggest investigating the UTR of
563 these DEGs as a potential region responsible for the non-coding function. With this approach, we
564 suggested another single-exon gene, *Sox11*, as a cncRNA gene regulating axon regeneration,
565 based on a retrospective re-analysis of our previously published dataset. *Sox11* is an injury-
566 responsive gene with a potential role in axon regeneration likely through its 5'UTR, while its protein
567 may employ different mechanisms in regulating regeneration. In addition, the 14-3-3 protein family
568 gene *Ywha-x* also exhibited features of a cncRNA. 14-3-3 proteins are known to play an important
569 role in regulating axon regeneration (Kaplan et al., 2017). In the present study, the 14-3-3 protein
570 family mRNA (*Ywha-x* mRNA) exhibited a dramatic release from CSDE1 when *Gpr151*-5'UTRm

571 was overexpressed, although the protein levels did not change (Supplementary information S6),
572 which suggests that this RNA may interact with RBPs other than ribosomes. This means that both
573 its protein and the mRNA itself are involved in the regulation of regeneration, though this needs to
574 be investigated further.

575 Our data show that expressing only the 5'UTR of *Gpr151* mRNA promotes peripheral axon
576 regeneration. In addition, overexpressing the engineered form of 5'UTR for enhanced CSDE1-
577 binding dramatically improves CNS axon regeneration in an optic nerve injury model. Therefore,
578 we present the engineered 5'UTR of *Gpr151* as a potential tool for the manipulation of the
579 regenerative potential of neurons. *Gpr151* mRNA is thus considered to be an RNA modulator that
580 regulates CSDE1-RNA interaction through its 5'UTR and that has a function that is distinct from its
581 protein in an axon regeneration paradigm.
582

Acknowledgements

We thank Dr. Aaron DiAntonio (Washington University in St. Louis) for critical reading of the manuscript. This work was supported by the Samsung Research Funding & Incubation Center of Samsung Electronics under Project Number SRFC-MA1802-07.

Author Contributions

Conceptualization, J.L., J.E.S., and Y.C.; Methodology, Formal Analysis, and Investigation, B.L., J.L., Y.J., H.K., M.K., J.E.S., and Y.C.; Resources, Funding Acquisition, Y.C.; Supervision and Project Administration, J.E.S. and Y.C.; Data Curation and Visualization, J.L., J.E.S., and Y.C.; Writing – Original Draft, B.L., J.L., Y.J., J.E.S., and Y.C.; Writing – Review & Editing, J.E.S. and Y.C.

Declaration of Interests

The authors declare no conflict of interest.

598 **Methods**

599 **Key Resources Table**

REAGENT or RESOURCE	SOURCE	IDENTIFIER
Antibodies		
Rabbit polyclonal Anti HA-ChIP Grade	Abcam	Cat#ab9110; RRID: AB_307019
Rabbit polyclonal Anti-GPR151	AVIVA SYSTEMS BIOLOGY	OAAF06441
Rat monoclonal Anti-alpha tublin(YOL1/34)	SANTA CRUZ BIOTECHNOLOGY	Cat#sc-53030; RRID: AB_2272440
Rabbit monoclonal Anti-c-Jun(60A8)	Cell Signaling Technology	Cat#9165s; RRID: AB_2130165
Rabbit polyclonal Anti-STMN2	Novus Biologicals	Cat#NBP1-49461; RRID: AB_10011569
Rabbit polyclonal Anti-Beta III tubulin	Abcam	Cat#ab18207; RRID:AB_444319
Chicken polyclonal Anti-Beta III tubulin	Abcam	Cat#ab41489; RRID: AB_727049
Mouse monoclonal Anti-GAPDH	SANTA CRUZ BIOTECHNOLOGY	Cat#sc-32233; RRID: AB_627679
Rabbit monoclonal Anti-DYKDDDDK tag(D6W5B)	Cell Signaling Technology Signaling	Cat#14793; RRID: AB_2572291
Goat anti-Mouse IgG (H+L) Secondary Antibody HRP conjugate	Thermo Fisher Scientific	Cat#62-6520; RRID: AB_2533947
Goat anti-Rabbit IgG (H+L) Secondary Antibody HRP conjugate	Thermo Fisher Scientific	Cat#65-6120; RRID: AB_2533967
Goat anti-Rabbit IgG (H+L) Secondary Antibody Alexa Fluor® 488 conjugate	Thermo Fisher Scientific	Cat#A-11034; RRID: AB_2576217
Goat Anti-Chicken IgY H&L (Alexa Fluor® 594) preadsorbed	abcam	Cat#ab150176; RRID: AB_2716250
Goat anti-Rabbit IgG (H+L) Secondary Antibody Alexa Fluor® 594 conjugate	Thermo Fisher Scientific	Cat#A-11037; RRID: AB_2534095
Goat anti-Rat IgG (H+L) Secondary Antibody HRP conjugate	Thermo Fisher Scientific	Cat#62-9520; RRID: AB_2533965
Bacterial and Virus Strains		

pAAV-shRNA-EGFP-U6-5'UTRm	Vectorbuilder	AAV9SP(VB181206-1015ysj)-C
Biological Samples		
Chemicals, Peptides, and Recombinant Proteins		
Vectashield antifade mounting medium	Vector Labs	Cat#H-1000; RRID: AB_2336789
Vectashield antifade mounting medium	Vector Labs	Cat#H-1200; RRID: AB_2336790
Dynabeads™ MyOne™ Streptavidin T1	Thermo Fisher Scientific	Cat#65601
cOmplete™, Mini, EDTA-free Protease Inhibitor Cocktail	Roche	Cat#4693159001
PhosSTOP™	Roche	Cat#4906837001
Cholera Toxin B Subunit	List biological	Cat#104
Critical Commercial Assays		
RNAscope Multiplex Fluorescent Reagent kit	ACD	Cat#320850
Lenti-X packaging Single Shots (Ecotropic)	Clontech	Cat#631276
cDNA-PCR sequencing kit	Oxford Nanopore Technologies	Cat#SQK-PCS109
Signaling explorer Antibody Array	ebiogen	Cat#SET100S
Phospho explorer Antibody Array	ebiogen	Cat#PEX100S
RNAqueous-Micro Total RNA isolation kit	Ambion	Cat#AM1931
Deposited Data		
Reference genome		
Raw data files for RNA-seq	This paper	
Experimental Models: Primary cultures		
Embryonic DRG neurons	This paper	Mouse: CD-1: Crl:CD1(ICR)
Experimental Models: Organisms/Strains		
Mouse: Advillin-Cre: *Avil*$^{tm2(cre)Fawa}$		JAX032536
Mouse: RiboTag: *Rpl22*$^{tm1.1Psam}$	The Jackson Laboratory	JAX029977
Mouse: KO: *Gpr151*^{tm1Dgen}	The Jackson Laboratory	JAX005805
Mouse: C57BL/6J: C57BL/6J	The Jackson Laboratory	JAX000664
Oligonucleotides		
siRNA targeting sequence: *Gpr151*: GCAAAGATTTCTGCTTTCAAA	TRC Library Database	TRCN0000026286
siRNA targeting sequence: *Csde1*: TGCTGTAAGTGCTCGTAATAT	TRC Library Database	TRCN0000276866
siRNA targeting sequence: *Khdrbs1*: GCATGTCTTCATTGAAGTCTT	TRC Library Database	TRCN0000102324

siRNA targeting sequence: *Jun*: CTCAACTGTGTAT GTACATAT	TRC Library Database	TRCN0000360500
siRNA targeting sequence: *Sox11*: TTCGACCTGAG CTTGAATTTC	TRC Library Database	TRCN0000365833
siRNA targeting sequence: *Ier5*: CCATCACTGTGG CCCAATATA	TRC Library Database	TRCN0000248616
qPCR primer		
Gpr151; Forward: CTGGGTTTGCCGACACCAAT, Reverse: AGAGAGACGGAATGATGGTCC	PrimerBank	33859815a1
Jun; Forward: CCTTCTACGACGATGCCCTC, Reverse: GGTTCAAGGTCATGCTCTGTTT	PrimerBank	6754402a1
Atf3; Forward: GAGGATTTTGCTAACCTGACACC, Reverse: TTGACGGTAACTGACTCCAGC	PrimerBank	31542154a1
RNA sequence(bait): 5'UTR of *Gpr151* - ΔCSDE1: CCAACCUAAAGCUACCAUCUGCAGGGAGGAGCUUG	This paper	N/A
RNA sequence(bait): 5'UTR of *Gpr151* - 4X mutant: ACAAGAAGACAAGAAGACAAGAAGACAAGAAG	This paper	N/A
RNA sequence(bait): 5'UTR of *GPR151* – human: CAAACCUAAAUAAGAAUCUAACUUCUGUAAGAAG CUGUGAAGAGUG	This paper	N/A
RNA sequence(bait): 5'UTR of *Gpr151* – mouse: CCAACCUAAACAAGAAGCUACCAUCUGCAGGGAG GAGCUUG	This paper	N/A
RNA sequence(bait): h of *Gpr151* – mouse: CCAACCUAAAC	This paper	N/A
RNA sequence(bait): 5'UTRm of *Gpr151* – mouse: CCAACCUAAACAAGAAGCUACCAUCUGCAGGGAG GUCGAAG	This paper	N/A
RNA sequence(bait): 5'UTR Δ of *Gpr151* – mouse: CCAACCUAAACAAGAAGC	This paper	N/A
Recombinant DNA		
Plasmid: FUGW-Flag-*Gpr151* (AUG->AUC point mutation)	This paper	N/A
Plasmid: FUGW-Flag- *Gpr151*	This paper	N/A
Plasmid: pLKO-5'UTR of *Sox11*	This paper	N/A
Software and Algorithms		
Samtools	Li et al., 2009	http://samtools.sourceforge.net/
ImageJ/Fiji for Mac	Schneider et al., 2012	https://imagej.nih.gov/ij/
Database for Annotation, Visualization and Integrated Discovery (DAVID)	Huang et al., 2009a, 2009b	https://david.ncifcrf.gov/tools.jsp
Origin	OriginLab	RRID:SCR_014212
Adobe Photoshop CC	Adobe	RRID:SCR_014199

minimap2	Li, 2018	doi:10.1093/bioinformatics/bty191

600

601 **Resource Availability**

602 **Lead Contact**

603 Further information and requests for reagents and resources should be directed to and will be
604 fulfilled by the lead contact, Yongcheol Cho (ycho77@korea.ac.kr).

605 **Materials Availability**

606 All materials used in this study are commercially available, as specified in the Key Resources Table.

607 **Data and Code Availability**

608 The dataset generated during this study are available at GEO XXXXXX.

609 **Experimental Model and Subject Details**

610 Primary embryonic DRG neuron cultures: DRG tissues from embryonic 13.5-days mice were
611 dissociated in 0.05% trypsin-EDTA (Thermo Fisher Scientific, 25300054) and plated on poly-D-
612 lysine (Sigma, P0899) / laminin (Thermo Fisher Scientific, 23017015)-coated dishes in Neurobasal
613 medium (Thermo Fisher Scientific, 21103049) supplemented with 2% B-27 (Thermo Fisher
614 Scientific, 17504044), 1% Glutamax (Thermo Fisher Scientific, 35050061), 1 μM 5-fluoro-2'-
615 deoxyuridine (Sigma, F0503), 1 μM uridine (Sigma, U3003), 1% penicillin-streptomycin (Thermo
616 Fisher Scientific, 15070063), and 50 ng/ml 2.5S nerve growth factor (Envigo, BT-5017). For the re-
617 plating assay, cultured neurons were replaced with DMEM (Hyclone, 500mlsh30243.01) / 0.05%
618 Trypsin-EDTA mixture (1:1) at DIV 5. Neurons were incubated in 37°C, 5% CO2 incubator for 5
619 min. Then, neurons were pipetted with culture medium described above. Cells were then
620 dissociated by gentle pipetting and transferred to new Lab-Tek chamber slides coated with poly-
621 D-lysine/laminin. After re-plating, neurons were incubated for 12~14 hours at 37°C with 5% CO2
622 then fixed in 4% paraformaldehyde (Biosesang, P2031) for 15min at room temperature. Neurite
623 lengths were measured and assessed using the Neurite Tracer for ImageJ

624 Animal models: (model organism: name used in paper: allele symbol) Mouse: RiboTag:
625 *Rpl22*$^{tm1.1Psam}$; Mouse: Advillin-Cre: *Avil*$^{tm2(cre)Fawa}$; Mouse: CD-1: Crl:CD1(ICR); Mouse: C57BL/6J:
626 C57BL/6J; Mouse: KO: *Gpr151*^{tm1Dgen}. For in vivo animal studies, all the experiments were carried

627 out in accordance with the Korea University Institutional Animal Care & Use Committee (KU-
628 IACUC). Mice were anesthetized using 3% isoflurane in oxygen until unresponsive to toe pinch to
629 confirm that the mouse is unconscious and kept on a heating pad for the duration of the surgery.
630 The surgery site was shaved and disinfected using organic iodine of chlorhexidine solution. All
631 surgery instruments were disinfected using autoclave and bead sterilizer. Mice were fed a diet
632 (PicoLab 5053, Purina) and maintained on a 12 hours light/dark cycle (6 am to 6 pm). Male and
633 female mice were housed in groups of up to 5 mice per cage. Age- and sex-matched male mice
634 were used at the indicated age. The *RiboTag* mouse carries a ribosomal protein gene with a floxed
635 C-terminal exon followed by an identical exon tagged with hemagglutinin (HA). When *RiboTag* is
636 crossed to a mouse expressing a cell-type-specific *Cre* recombinase, expression of the epitope-
637 tagged protein is activated in the cell type of interest. A homozygote *RiboTag* mice (*Rpl22HA*)
638 obtained from Jackson Laboratory and *Advillin-Cre* driver line (Hasegawa et al., 2007) were
639 crossed. *Cre* positive RiboTag animals (*Rpl22HA*+/+; advillin-Cre+/-) and the littermate control
640 (*Rpl22HA* +/+; advillin-Cre-/-) mice were generated by crossing *Rpl22HA* +/+; advillin-Cre+/- male
641 with *Rpl22HA* +/+ female. Three-months or older mice were used for sciatic nerve transection
642 surgery. Mice sciatic nerve was unilaterally exposed through a small incision made to the skin and
643 muscles at mid-thigh level. Then, the sciatic nerve was transected by surgical scissors and the
644 incision was closed by nylon suture. The animals were then subjected to post-operation care until
645 euthanized for analysis.

646 **Method Details**

647 **Gene delivery using virus**

648 Lentivirus-mediated gene delivery was used for knocking down the target mRNA or overexpressing
649 exogenous genes from the embryonic DRG neurons. Lentivirus was produced with Lenti-X
650 packaging Single Shots (Takara, 631275) as following the manual. For in vitro gene delivery,
651 lentivirus was applied to the embryonic DRG neuron cultures at DIV 2. To deliver genes in vivo,
652 adeno-associated virus (AAV, serotype 9) (10μl) was injected to neonatal CD-1 mice (postnatal
653 day 1) by facial vein injection using a Hamilton syringe (Hamilton, 1710 syringe with 33G/0.75-inch

654 small hub removable needle). 10μl of AAV virus was tested and the expression of GFP and target
655 genes in sciatic nerve and DRG was confirmed by immunohistochemistry and RT-qPCR analysis.

656 **Antibody array**

657 Embryonic DRG neurons were rinsed with 1X PBS then collected by gentle centrifugation. The cell
658 pellet was collected at DIV 6. Frozen pellets of eDRG cells were sent to ebiogen (Seoul, South
659 Korea) who carried out antibody array and initial data analyses. The Signaling Explorer Antibody
660 Microarray (SET100) consisting of 1,358 antibodies were supplied by Full Moon BioSystems, Inc.,
661 (Sunnyvale, CA, USA).

662 **Ribosome-associated RNA seq**

663 At 24 h after nerve lesion, L4,5 DRG tissues were dissected from both *Cre*-positive and negative
664 *RiboTag* mice. Tissues were homogenized in lysis buffer (1% NP-40, 20mM HEPES-KOH, 5mM
665 $MgCl_2$, 150mM KCl, 1mM DTT, SUPERase In (Thermo Fisher Scientific, AM2694), and Complete
666 EDTA-free Protease Inhibitor Cocktail (Sigma, 11873580001)) in the presence of cycloheximide
667 (Sigma, C7698-1G), rapamycin (Sigma, R0395), then post-mitochondrial fractions were collected.
668 We followed the TRAP protocol as described (Shigeoka et al., 2016). Pre-cleared ribosome-mRNA
669 complexes were immunoprecipitated by an anti-HA antibody and Dynabeads Protein G (Thermo
670 Fisher Scientific, 10004D). Total RNA was extracted from the ribosome-mRNA complexes using a
671 RNeasy mini kit (Qiagen, 217084) followed by in-column DNase treatment to remove genomic
672 DNA contamination. The RNA samples were examined for quantity and quality using Nanodrop.

673 **Immunoprecipitating RNA binding proteins**

674 At 24 h after nerve lesion, L4,5 DRG tissues were dissected from mice. Tissues were homogenized
675 in TRAP lysis buffer. CSDE1 was immunoprecipitated by anti-CSDE1 antibody pre-bound to
676 Dynabeads Protein G (Thermo Fisher Scientific, 10004D) from total 82 μg input lysates for 16
677 hours at 4'C. The precipitants were washed 5-times using DynaMag-2 (Thermo Fisher Scientific,
678 12321D) and subjected to reverse transcription for quantitative real time PCR.

679 **Library preparation and nanopore sequencing analysis**

680 Nanopore libraries were prepared from total RNA combined using the nanopore PCR cDNA
681 sequencing Kit (SQK-PCS109, Oxford Nanopore Technologies) according to manufacturer's

682 instructions. The VN primer was annealed to the RNA to target poly A tail, then first-strand cDNA
683 was synthesized by Maxima H Minus Reverse Transcriptase (Thermo Fisher Scientific, EP0752).
684 The RNA-cDNA hybrid was then purified using Agencourt AMPure XP magnetic beads (Beckman
685 Coulter, A63880). PCR was performed using 2x LongAmp Taq Master Mix (New England Biolabs,
686 M0287S) to select full-length transcripts followed by a second purification step using Agencourt
687 beads (as described above). The purified cDNA was resuspended by adding 12 µl Elution Buffer
688 and resuspending the beads, incubating at room temperature for 10 min, pelleting the beads again,
689 and transferring the supernatant (pre-sequencing mix) to a new tube. Then the Rapid Adapter was
690 ligated to the cDNA library. Nanopore sequencing was performed as per manufacturer's guidelines
691 using R9.4 SpotON flow cells (FLO-MIN106, ONT) with MinION sequencer. MinION sequencing
692 was controlled using Oxford Nanopore Technologies MinKNOW software as following the manual.
693 Following basecalling, nanopore read data were aligned to the *Mus musculus* reference
694 (GRCm38.p6, GCA_000001635.8) and transcriptome using MiniMap2. Note that following
695 mapping, all SAM files were parsed to sorted BAM files using SAMtools v1.3.1. For direct RNA
696 sequencing, libraries were prepared from total RNA by using the Nanopore Direct RNA sequencing
697 Kit (SQK-RNA002, Oxford Nanopore Technologies) according to manufacturer's instructions. The
698 RT adapter was annealed to the RNA for reverse transcription, then reverse-transcribed RNA was
699 then purified using Agencourt RNAClean XP magnetic beads (Beckman Coulter, A63880). The
700 purified RNA was eluted from the RNAClean beads (included in the kit) in 21µl Elution Buffer
701 included in the kit. Then the Sequencing Adapter was ligated to the library.

702 **PNS axon regeneration assay**

703 For pre-conditioning injury, the right sciatic nerve of age- and sex-matched mice was crushed by
704 forceps and L4,5 DRGs were dissected from spinal cord at the indicated days after injury. Adult
705 DRGs were dissociated using Liberase TM (Roche, 5401119001), DNase I (Sigma, 11284932001)
706 and bovine serum albumin (Sigma, A2153) and trypsin-EDTA for 15 min in each condition at 37°C.
707 Dissociated DRGs were triturated gently by pipetting and plated in DMEM (Hyclone,
708 500mlsh30243.01) with 10% FBS (Thermo Fisher Scientific, 16000044), 1% penicillin-
709 streptomycin, (Thermo Fisher Scientific, 15070063) and 1% Glutamax (Thermo Fisher Scientific,

710 35050061) on culture dishes coated with poly-D-lysine (Sigma, P0899) and laminin (Thermo Fisher
711 Scientific, 23017015), incubated in humidified 37'C / 5% CO_2 incubator. Sciatic nerves were
712 dissected at 3 days after crush injury and dissected, sectioned and immunostained with TUJ1
713 antibody and anti-SCG10 antibody. To visualize the regenerating axons in a single image, multiple
714 pictures were taken along the nerve and montaged automatically in microscope (EVOS FL Auto
715 Cell Imaging System, Thermo Fisher Scientific, AMC1000). SCG10 fluorescence intensity was
716 measured along the length of the nerve sections using ImageJ software. An SCG10 intensity plot
717 was drawn with average intensities calculated from 50 pixels. A regeneration index was calculated
718 by measuring the average SCG10 intensity from the injury site to the distal side, which is defined
719 by the position along the nerve length with maximal SCG10 intensity, correlating with TUJ1 labeling
720 where deformation of the nerve and disruption of axons are identified.

721 **CNS axon regeneration assay**

722 For CNS axon regeneration assay in vivo from optic nerve injury model, 1.5 ul of AAV was injected
723 with pulled glass needle to vitreous of eye. The conjunctiva from the orbital part of the eye was
724 cleared in order to expose the optic nerve, which was crushed for 3 seconds with Dumont #5
725 forceps (Fine Science Tools, 11254-20) and special care was taken not to damage the vein sinus.
726 To avoid desiccation of the eye, a saline solution was applied before and after optic nerve crush.
727 For cholera toxin b (CTB) axon tracing, 1% atropine sulfate solution (Bauch & Lomb) was applied
728 to the eye to induce pupil dilation. A pulled glass needle was introduced in the vitreous through the
729 ora serrate and 2μl of 2μg/μl CTB (Thermo Fisher Scientific, C34777) was injected. For optic nerve
730 fixation and sectioning, mice were sacrificed at two days after CTB injection and eyes and optic
731 nerves altogether were fixed by immersion in 4% paraformaldehyde solution for 2 hours. After
732 being washed three times in PBS, eyes were transferred to 30% sucrose solution for 24 hours at
733 4'C. Optic nerves were then dissected out with micro scissors (Fine Science Tools, 15070-08),
734 sectioned at 11μm in the cryostat and mounted in mounting medium ProLong Gold (Thermo Fisher
735 Scientific, P36931). Optic nerve sections were imaged with EVOS FL Auto Cell Imaging System.
736 Numbers of regenerating axons at different distances from the injury site were estimated following
737 the published protocol described by Park et al., 2008. The numbers of regenerating axons crossing

738 lines set at 0.2, 0.5, 0.8 and 1mm from the injury site were quantified in 5 different slices per optic
739 nerve using ImageJ. The cross-sectional width of the optic nerve was used to estimate the number
740 of regenerating axons per μm. The total number of regenerating axons per each optic nerve at
741 certain distance from the injury site (Σa_d) was estimated using the following formula: $\Sigma a_d = \pi$ x
742 (optic nerve radius)^2 x [average axons/μm] / 11μm. For statistical analysis, the numbers of
743 regenerating axons from control and 5'UTRm-expressing mice at each distance were compared
744 using Student's t test.

745 **Fluorescent in situ hybridization**

746 *Gpr151* RNA was detected by a pair of target probe (RNAscope Probe-Mm-*Gpr151*, ACD, 317321)
747 following the manufacture's instructions. L4,5 DRG tissues were fixed in 4% paraformaldehyde
748 and permeabilized. The fixed sample tissues were cryo-blocked with OCT compound and
749 sectioned at a 10μm thickness with cryotome. The sections were dehydrated with 50%, 70% to
750 100% Ethanol for 5min each at room temperature, followed by air dry for 5 min at room temperature.
751 Tissue section was incubated in Protease 4 (ACD, from the kit RNAscope, 322000) solution for 15
752 min at room temperature. To wash, phosphate-buffered saline was applied five times to the tissue
753 section. Target probe was pre-warmed at 40'C and then the probe was applied to tissue section
754 and incubated for 2 hours in 40'C. Slide was then washed by wash buffer (ACD, from the kit
755 RNAscope, 322000) twice. The fluorescence probes Amp-1-FL, Amp-2-FL and Amp3-FL were
756 applied to tissue section for 30 min at 40'C. Finally, Amp-4-FL was applied and incubated for 15
757 min at 40'C. The prepared samples were mounted and analyzed under confocal microscope (Zeiss,
758 LSM700).

759 **Biotin-RNA pull down assay and mass spectrometry analysis**

760 All the RNA baits used for pull-down assay were synthesized by IDT. Total protein lysates were
761 prepared from DRG tissues dissected from 6-weeks old CD-1 mice, lysed in lysis buffer (1% NP-
762 40, 20mM HEPES-KOH, 5mM $MgCl_2$, 150mM KCl, 1mM DTT, SUPERase In (Thermo Fisher
763 Scientific, AM2694), and Complete EDTA-free Protease Inhibitor Cocktail (Sigma, 11873580001)).
764 1 mg of protein lysates was subjected as an input for each pull-down condition. The quantified
765 protein input was incubated with the indicated biotin-RNA baits for 16 hours at 4'C, followed by

766 incubation with Dynabeads MyOne Streptavidin T1 (Thermo Fisher Scientific, 65601) for additional
767 1 hour at 4'C with rotation. The magnetic beads complexes were washed and recovered by magnet
768 (Thermo Fisher Scientific, 12321D) as following the manufacturer's instructions. Total protein from
769 the precipitated magnetic beads were eluted by incubating at 95'C for 10 min in 1X SDS-PAGE
770 sampling buffer then subjected to SDS-PAGE separation. For identifying the eluted proteins by
771 mass spectrometry analysis, protein bands from PAGE gel were visualized by Coomassie staining
772 method and sliced to subject to in-gel digestion. All the mass spectrometry analysis including
773 sample preparation were done by YPRC (Yonsei Proteome Research Center, Seoul Korea).

774 **Supplementary information**

775 **Supplementary figure 1.** Western blot analysis of L4,L5 DRG tissues dissected from *RiboTag* x
776 *Advillin*-Cre mice with (+Injury) or without (-Injury) sciatic nerve axotomy. Anti-HA epitope antibody
777 was used to detect RPL22HA protein, related to figure 1A.

778 **Supplementary figure 2.** Visualization of the illumina sequencing results mapped with mouse
779 *Gpr151* gene using *SeqMonk*.

780 **Supplementary figure 3.** In vitro axon regeneration assay. (A) Representative images of control,
781 5'UTRm-overexpressing, and 5'UTRm ΔCSDE1-overexpressing embryonic DRG neurons. Scale
782 bar, 100 μm. (B) Statistical analysis of regenerating axon length of (A) (n=254, 198, 167 for control,
783 shCSDE1 and shKHDRBS1; ***p<0.001, ns, not significant by ANOVA followed by Tukey tests;
784 mean±SEM). (B) Statistics of average of relative axon length of (A) (n=64, 55, 68 cells for control,
785 5'UTRm, 5'UTRm ΔCSDE1; **p*<0.05, ns, not significant by ANOVA followed by Tukey tests;
786 mean±SEM), related to figure 5A.

787 **Supplementary figure 4.** Statistical analysis of regenerating axon length of embryonic neurons of
788 control, sh*Ier5*, sh*Jun*, sh*Sox11* (n=156, 79, 78, 45 for each condition; ***p<0.001, ns, not
789 significant by ANOVA followed by Tukey tests; mean±SEM), related to figure 7A.

790 **Information S1.** The list of identified peptides by mass spectrophotometry analysis of figure 4A.

791 **Information S2.** CSDE1 IP-sequencing result, related to figure 5C.

792 **Information S3.** Gene ontology analysis of figure 5D.

793 **Information S4.** KEGG pathway analysis of figure 5E.

794 **Information S5.** Antibody array analysis of figure 5F.

795 **Information S6.** Comparative analysis between CSDE1 IP-seq and antibody array analysis of
796 figure 5G.

797

798

References

Antolin-fontes, B., Li, K., Ables, J.L., Riad, M.H., Görlich, A., Williams, M., Wang, C., Lipford, S.M., Dao, M., Molina, H., et al. (2019). Across Drug Classes.

Antolin-Fontes, B., Li, K., Ables, J.L., Riad, M.H., Görlich, A., Williams, M., Wang, C., Lipford, S.M., Dao, M., Liu, J., et al. (2020). The habenular G-protein–coupled receptor 151 regulates synaptic plasticity and nicotine intake. Proc. Natl. Acad. Sci. U. S. A. *117*, 5502–5509.

Blackmore, M.G. (2012). Molecular Control of Axon Growth: Insights from Comparative Gene Profiling and High-Throughput Screening (Elsevier Inc.).

Boulos, L.J., Darcq, E., and Kieffer, B.L. (2017). Translating the Habenula—From Rodents to Humans. Biol. Psychiatry *81*, 296–305.

Broms, J., Antolin-Fontes, B., Tingström, A., and Ibañez-Tallon, I. (2015). Conserved expression of the GPR151 receptor in habenular axonal projections of vertebrates. J. Comp. Neurol. *523*, 359–380.

Broms, J., Grahm, M., Haugegaard, L., Blom, T., Meletis, K., and Tingström, A. (2017). Monosynaptic retrograde tracing of neurons expressing the G-protein coupled receptor Gpr151 in the mouse brain. J. Comp. Neurol. *525*, 3227–3250.

Chen, L., Liu, Z., Zhou, B., Wei, C., Zhou, Y., Rosenfeld, M.G., Fu, X.D., Chisholm, A.D., and Jin, Y. (2016). CELF RNA binding proteins promote axon regeneration in C. elegans and mammals through alternative splicing of syntaxins. Elife *5*, 1–26.

Conlon, E.G., and Manley, J.L. (2017). RNA-binding proteins in neurodegeneration: Mechanisms in aggregate. Genes Dev. *31*, 1509–1528.

Curcio, M., and Bradke, F. (2018). Axon Regeneration in the Central Nervous System: Facing the Challenges from the Inside. Annu. Rev. Cell Dev. Biol. *34*, 495–521.

Dennis, G., Sherman, B.T., Hosack, D.A., Yang, J., Gao, W., Lane, H.C., and Lempicki, R.A. (2003). DAVID: Database for Annotation, Visualization, and Integrated Discovery. Genome Biol. *4*.

Donnelly, C.J., Willis, D.E., Xu, M., Tep, C., Jiang, C., Yoo, S., Schanen, N.C., Kirn-Safran, C.B., Van Minnen, J., English, A., et al. (2011). Limited availability of ZBP1 restricts axonal mRNA localization and nerve regeneration capacity. EMBO J. *30*, 4665–4677.

Dulin, J.N., Antunes-Martins, A., Chandran, V., Costigan, M., Lerch, J.K., Willis, D.E., and Tuszynski, M.H. (2015). Transcriptomic Approaches to Neural Repair. J. Neurosci. *35*, 13860–13867.

Le Foll, B., and French, L. (2018). Transcriptomic Characterization of the Human Habenula Highlights

829 Drug Metabolism and the Neuroimmune System. Front. Neurosci. *12*, 1–16.
830 Förstner, P., Rehman, R., Anastasiadou, S., Haffner-Luntzer, M., Sinske, D., Ignatius, A., Roselli, F.,
831 and Knöll, B. (2018). Neuroinflammation after Traumatic Brain Injury Is Enhanced in Activating
832 Transcription Factor 3 Mutant Mice. J. Neurotrauma *35*, 2317–2329.
833 Gopal, P.P., Nirschl, J.J., Klinman, E., and Holzbaurb, E.L.F. (2017). Amyotrophic lateral sclerosis-
834 linked mutations increase the viscosity of liquid-like TDP-43 RNP granules in neurons. Proc. Natl.
835 Acad. Sci. U. S. A. *114*, E2466–E2475.
836 Gorlich, A., Antolin-Fontes, B., Ables, J.L., Frahm, S., Slimak, M.A., Dougherty, J.D., and Ibanez-
837 Tallon, I. (2013). Reexposure to nicotine during withdrawal increases the pacemaking activity of
838 cholinergic habenular neurons. Proc. Natl. Acad. Sci. *110*, 17077–17082.
839 Gunawardana, Y., and Niranjan, M. (2013). Bridging the gap between transcriptome and proteome
840 measurements identifies post-translationally regulated genes. Bioinformatics *29*, 3060–3066.
841 Guo, H., Li, Y., Shen, L., Wang, T., Jia, X., Liu, L., Xu, T., Ou, M., Hoekzema, K., Wu, H., et al.
842 (2019). Disruptive variants of CSDE1 associate with autism and interfere with neuronal development
843 and synaptic transmission. Sci. Adv. *5*, 1–17.
844 Gygi, S.P., Rochon, Y., Franza, B.R., and Aebersold, R. (1999). Correlation between Protein and
845 mRNA Abundance in Yeast. Mol. Cell. Biol. *19*, 1720–1730.
846 He, Z., and Jin, Y. (2016). Intrinsic Control of Axon Regeneration. Neuron *90*, 437–451.
847 Hentze, M.W., Castello, A., Schwarzl, T., and Preiss, T. (2018). A brave new world of RNA-binding
848 proteins. Nat. Rev. Mol. Cell Biol. *19*, 327–341.
849 Holmes, F.E., Kerr, N., Chen, Y.J., Vanderplank, P., McArdle, C.A., and Wynick, D. (2017). Targeted
850 disruption of the orphan receptor Gpr151 does not alter pain-related behaviour despite a strong
851 induction in dorsal root ganglion expression in a model of neuropathic pain. Mol. Cell. Neurosci. *78*,
852 35–40.
853 Hörnberg, H., and Holt, C. (2013). RNA-binding proteins and translational regulation in axons and
854 growth cones. Front. Neurosci. *7*, 1–9.
855 Hosack, D.A., Dennis, G., Sherman, B.T., Lane, H.C., and Lempicki, R.A. (2003). Identifying
856 biological themes within lists of genes with EASE. Genome Biol. *4*.
857 Huang, D.W., Sherman, B.T., and Lempicki, R.A. (2009). Systematic and integrative analysis of large
858 gene lists using DAVID bioinformatics resources. Nat. Protoc. *4*, 44–57.

859 Jankowski, M.P., Miller, L., and Koerber, H.R. (2018). Increased Expression of Transcription Factor
860 SRY-box-Containing Gene 11 (Sox11) Enhances Neurite Growth by Regulating Neurotrophic Factor
861 Responsiveness. Neuroscience *382*, 93–104.
862 Jiang, B.-C., Sun, W.-X., He, L.-N., Cao, D.-L., Zhang, Z.-J., and Gao, Y.-J. (2015). Identification of
863 lncRNA Expression Profile in the Spinal Cord of Mice following Spinal Nerve Ligation-Induced
864 Neuropathic Pain. Mol. Pain *11*, s12990-015–0047.
865 Jiang, B.-C., Zhang, W.-W., Yang, T., Guo, C.-Y., Cao, D.-L., Zhang, Z.-J., and Gao, Y.-J. (2018a).
866 Demethylation of G-Protein-Coupled Receptor 151 Promoter Facilitates the Binding of Krüppel-Like
867 Factor 5 and Enhances Neuropathic Pain after Nerve Injury in Mice. J. Neurosci. *38*, 10535–10551.
868 Jiang, B.C., Zhang, W.W., Yang, T., Guo, C.Y., Cao, D.L., Zhang, Z.J., and Gao, Y.J. (2018b).
869 Demethylation of G-protein-coupled receptor 151 promoter facilitates the binding of Krüppel-like factor
870 5 and enhances neuropathic pain after nerve injury in mice. J. Neurosci. *38*, 10535–10551.
871 Ju Lee, H., Bartsch, D., Xiao, C., Guerrero, S., Ahuja, G., Schindler, C., Moresco, J.J., Yates, J.R.,
872 Gebauer, F., Bazzi, H., et al. (2017). A post-transcriptional program coordinated by CSDE1 prevents
873 intrinsic neural differentiation of human embryonic stem cells. Nat. Commun. *8*.
874 Kaplan, A., Morquette, B., Kroner, A., Leong, S.Y., Madwar, C., Sanz, R., Banerjee, S.L., Antel, J.,
875 Bisson, N., David, S., et al. (2017). Small-Molecule Stabilization of 14-3-3 Protein-Protein Interactions
876 Stimulates Axon Regeneration. Neuron *93*, 1082-1093.e5.
877 Kong, G., Zhou, L., Serger, E., Palmisano, I., De Virgiliis, F., Hutson, T.H., Mclachlan, E., Freiwald,
878 A., La Montanara, P., Shkura, K., et al. (2020). AMPK controls the axonal regenerative ability of
879 dorsal root ganglia sensory neurons after spinal cord injury. Nat. Metab. *2*, 918–933.
880 Koussounadis, A., Langdon, S.P., Um, I.H., Harrison, D.J., and Smith, V.A. (2015). Relationship
881 between differentially expressed mRNA and mRNA-protein correlations in a xenograft model system.
882 Sci. Rep. *5*, 1–9.
883 Kumari, P., and Sampath, K. (2015). CncRNAs: Bi-functional RNAs with protein coding and non-
884 coding functions. Semin. Cell Dev. Biol. *47–48*, 40–51.
885 Li, Y., Struebing, F.L., Wang, J., King, R., and Geisert, E.E. (2018). Different Effect of Sox11 in
886 Retinal Ganglion Cells Survival and Axon Regeneration. Front. Genet. *9*, 1–14.
887 Liu, K., Tedeschi, A., Park, K.K., and He, Z. (2011). Neuronal Intrinsic Mechanisms of Axon
888 Regeneration. Annu. Rev. Neurosci. *34*, 131–152.

889 Liu, Y., Beyer, A., and Aebersold, R. (2016). On the Dependency of Cellular Protein Levels on mRNA
890 Abundance. Cell *165*, 535–550.
891 Ma, T.C., and Willis, D.E. (2015). What makes a RAG regeneration associated? Front. Mol. Neurosci.
892 *8*, 1–13.
893 Mahar, M., and Cavalli, V. (2018a). Intrinsic mechanisms of neuronal axon regeneration. Nat. Rev.
894 Neurosci. *19*, 323–337.
895 Mahar, M., and Cavalli, V. (2018b). Intrinsic mechanisms of neuronal axon regeneration. Nat. Rev.
896 Neurosci. *19*, 323–337.
897 Maier, T., Güell, M., and Serrano, L. (2009). Correlation of mRNA and protein in complex biological
898 samples. FEBS Lett. *583*, 3966–3973.
899 Marvaldi, L., Panayotis, N., Alber, S., Dagan, S.Y., Okladnikov, N., Koppel, I., Di Pizio, A., Song, D.,
900 Tzur, Y., Terenzio, M., et al. (2020). Importin α3 regulates chronic pain pathways in peripheral
901 sensory neurons. Science (80-.). *369*, 842–846.
902 Michaelevski, I., Segal-Ruder, Y., Rozenbaum, M., Medzihradszky, K.F., Shalem, O., Coppola, G.,
903 Horn-Saban, S., Ben-Yaakov, K., Dagan, S.Y., Rishal, I., et al. (2010). Signaling to transcription
904 networks in the neuronal retrograde injury response. Sci. Signal. *3*.
905 Moore, K.S., Yagci, N., Van Alphen, F., Paolini, N.A., Horos, R., Held, N.M., Houtkooper, R.H., Van
906 Den Akker, E., Meijer, A.B., T'Hoen, P.A.C., et al. (2018). Csde1 binds transcripts involved in protein
907 homeostasis and controls their expression in an erythroid cell line. Sci. Rep. *8*, 1–14.
908 Norsworthy, M.W., Bei, F., Kawaguchi, R., Wang, Q., Tran, N.M., Li, Y., Brommer, B., Zhang, Y.,
909 Wang, C., Sanes, J.R., et al. (2017). Sox11 Expression Promotes Regeneration of Some Retinal
910 Ganglion Cell Types but Kills Others. Neuron *94*, 1112-1120.e4.
911 Van Nostrand, E.L., Freese, P., Pratt, G.A., Wang, X., Wei, X., Xiao, R., Blue, S.M., Chen, J.-Y.,
912 Cody, N.A.L., Dominguez, D., et al. (2020). A large-scale binding and functional map of human RNA-
913 binding proteins. Nature *583*, 711–719.
914 Nussbacher, J.K., Batra, R., Lagier-Tourenne, C., and Yeo, G.W. (2015). RNA-binding proteins in
915 neurodegeneration: Seq and you shall receive. Trends Neurosci. *38*, 226–236.
916 Reinhold, A.K., Batti, L., Bilbao, D., Buness, A., Rittner, H.L., and Heppenstall, P.A. (2015).
917 Differential transcriptional profiling of damaged and intact adjacent dorsal root ganglia neurons in
918 neuropathic pain differential transcriptional profiling of damaged and intact adjacent dorsal root

919 ganglia neurons in neuropathic pain. PLoS One *10*, 1–17.
920 Saltel, F., Giese, A., Azzi, L., Elatmani, H., Costet, P., Ezzoukhry, Z., Dugot-Senant, N., Miquerol, L.,
921 Boussadia, O., Wodrich, H., et al. (2017). Unr defines a novel class of nucleoplasmic reticulum
922 involved in mRNA translation. J. Cell Sci. *130*, 1796–1808.
923 Sampath, K., and Ephrussi, A. (2016). CncRNAs: RNAs with both coding and non-coding roles in
924 development. Development *143*, 1234–1241.
925 Sanz, E., Yang, L., Su, T., Morris, D.R., McKnight, G.S., and Amieux, P.S. (2009). Cell-type-specific
926 isolation of ribosome-associated mRNA from complex tissues. Proc. Natl. Acad. Sci. U. S. A. *106*,
927 13939–13944.
928 Sherman, B.T., Huang, D.W., Tan, Q., Guo, Y., Bour, S., Liu, D., Stephens, R., Baseler, M.W., Lane,
929 C.H., and Lempicki, R.A. (2007). DAVID Knowledgebase: A gene-centered database integrating
930 heterogeneous gene annotation resources to facilitate high-throughput gene functional analysis. BMC
931 Bioinformatics *8*, 1–11.
932 Shigeoka, T., Jung, H., Jung, J., Turner-Bridger, B., Ohk, J., Lin, J.Q., Amieux, P.S., and Holt, C.E.
933 (2016). Dynamic Axonal Translation in Developing and Mature Visual Circuits. Cell *166*, 181–192.
934 Shin, J.E., and Cho, Y. (2017). Epigenetic Regulation of Axon Regeneration after Neural Injury. Mol.
935 Cells *40*, 10–16.
936 Shin, J.E., Miller, B.R., Babetto, E., Cho, Y., Sasaki, Y., Qayum, S., Russler, E. V, Cavalli, V.,
937 Milbrandt, J., and DiAntonio, A. (2012a). SCG10 is a JNK target in the axonal degeneration pathway.
938 Proc. Natl. Acad. Sci. U. S. A. *109*, E3696-705.
939 Shin, J.E., Cho, Y., Beirowski, B., Milbrandt, J., Cavalli, V., and DiAntonio, A. (2012b). Dual Leucine
940 Zipper Kinase Is Required for Retrograde Injury Signaling and Axonal Regeneration. Neuron *74*,
941 1015–1022.
942 Shin, J.E., Geisler, S., and DiAntonio, A. (2014). Dynamic regulation of SCG10 in regenerating axons
943 after injury. Exp. Neurol. *252*, 1–11.
944 Shin, J.E., Ha, H., Cho, E.H., Kim, Y.K., and Cho, Y. (2018). Comparative analysis of the
945 transcriptome of injured nerve segments reveals spatiotemporal responses to neural damage in mice.
946 J. Comp. Neurol. *526*, 1195–1208.
947 Shin, J.E., Ha, H., Kim, Y.K., Cho, Y., and DiAntonio, A. (2019). DLK regulates a distinctive
948 transcriptional regeneration program after peripheral nerve injury. Neurobiol. Dis. *127*, 178–192.

949 Smith, D.S., and Skene, J.H. (1997). A transcription-dependent switch controls competence of adult
950 neurons for distinct modes of axon growth. J. Neurosci. *17*, 646–658.
951 Stein, L.M., Yosten, G.L.C., and Samson, W.K. (2016). Adropin acts in brain to inhibit water drinking:
952 potential interaction with the orphan G protein-coupled receptor, GPR19. Am. J. Physiol. Integr.
953 Comp. Physiol. *310*, R476–R480.
954 Stern, S., Sinske, D., and Knöll, B. (2012). Serum response factor modulates neuron survival during
955 peripheral axon injury. J. Neuroinflammation *9*, 1–12.
956 Sun, F., and He, Z. (2010). Neuronal intrinsic barriers for axon regeneration in the adult CNS. Curr.
957 Opin. Neurobiol. *20*, 510–518.
958 Tedeschi, A., and Popovich, P.G. (2019). The application of omics technologies to study axon
959 regeneration and CNS Repair [version 1; peer review: 3 approved]. F1000Research *8*, 1–13.
960 Tedeschi, A., Omura, T., and Costigan, M. (2017). CNS repair and axon regeneration: Using genetic
961 variation to determine mechanisms. Exp. Neurol. *287*, 409–422.
962 Terman, S.A. (1970). Relative effect of transcription-level and translation-level control of protein
963 synthesis during early development of the sea urchin. Proc. Natl. Acad. Sci. U. S. A. *65*, 985–992.
964 Triqueneaux, G., Velten, M., Franzon, P., Dautry, F., and Jacquemin-Sablon, H. (1999). RNA binding
965 specificity of Unr, a protein with five cold shock domains. Nucleic Acids Res. *27*, 1926–1934.
966 Wlaschin, J.J., Gluski, J.M., Nguyen, E., Silberberg, H., Thompson, J.H., Chesler, A.T., and Le
967 Pichon, C.E. (2018). Dual leucine zipper Kinase is required for mechanical allodynia and microgliosis
968 after nerve injury. Elife *7*, 1–19.
969 Wu, S., Marie Lutz, B., Miao, X., Liang, L., Mo, K., Chang, Y.J., Du, P., Soteropoulos, P., Tian, B.,
970 Kaufman, A.G., et al. (2016). Dorsal root ganglion transcriptome analysis following peripheral nerve
971 injury in mice. Mol. Pain *12*, 1–14.
972 Wurth, L., Papasaikas, P., Olmeda, D., Bley, N., Calvo, G.T., Guerrero, S., Cerezo-Wallis, D.,
973 Martinez-Useros, J., García-Fernández, M., Hüttelmaier, S., et al. (2016). UNR/CSDE1 Drives a Post-
974 transcriptional Program to Promote Melanoma Invasion and Metastasis. Cancer Cell *30*, 694–707.
975 Zurborg, S., Piszczek, A., Martínez, C., Hublitz, P., Al Banchaabouchi, M., Moreira, P., Perlas, E., and
976 Heppenstall, P.A. (2011). Generation and characterization of an Advillin-Cre driver mouse line. Mol.
977 Pain *7*, 1–10.
978